IMPACT INVESTIGATION USING ANSYS AUTODYN CODE ON A REINFORCED

CONCRETE MODEL DUE TO TNT SHAPED CHARGE FOR NUCLEAR SECURITY

VULNERABILITY ASSESSMENTS

A Thesis

by

JEEHOON MOO

Submitted to the Office of Graduate and Professional Studies of
Texas A&M University
in partial fulfillment of the requirements for the degree of

MASTER OF SCIENCE

Chair of Committee,	Sunil S. Chirayath
Committee Members,	Pavel V. Tsvetkov
	Joseph M. Bracci
Head of Department,	John E. Hurtado

May 2019

Major Subject: Nuclear Engineering

ABSTRACT

The objective of this study is to predict the damage that could be created on a reinforced concrete wall due to the impact of Tri-Nitro Toluene (TNT) shaped charge using a numerical simulation software. There are many commercial numerical simulation software that can be used to solve engineering problems in real world scenarios, such as ANSYS, ABAQUS, LS-DYNA, etc. ANSYS Simulation Software is one of the strongest and user-friendly commercial finite element analysis (FEA) tools that uses computer-based numerical techniques.

In this study, two different types of simulation software codes which can be coupled for the advanced analysis are used within ANSYS Simulation Software system. One is ANSYS Explicit Dynamic STR (Structure) software and the other one is ANSYS AUTODYN software. ANSYS Explicit Dynamic STR software provides suitable solutions of nonlinear dynamic events for a short duration, including a drop and impact testing with low velocity or high velocity, deformation by high pressure, explosion, etc. ANSYS AUTODYN software also provides suitable solutions of nonlinear dynamic events similar to ANSYS Explicit Dynamic STR, but this software is focused on complicated nonlinear dynamic events like high explosions and detailed damage responses of materials such as cracks and fragments.

The reinforced concrete wall target is located at a distance of 50 meters from a TNT shaped charge design. Various TNT shaped charge designs are studied by changing the amount of TNT and liner fragment thickness, etc. in order to make the hole-size big enough on the concrete wall target so that at least a person can pass through it at a time.

In addition, a physical protection system vulnerability assessment is performed with a hypothetic nuclear research reactor assuming that TNT shaped charge is used in order to reach to a desired target from the offsite to the nuclear research reactor. The probability of interruption (P_I) is calculated with the Adversary Sequence Diagram (ASD) using Estimate of Adversary Sequence Interruption (EASI) model to conduct the vulnerability assessment, which provides the most vulnerable paths to reach to the target while minimizing time delay (t_D) and the probability of detection (P_D).

ACKNOWLEDGEMENTS

I would like to thank my committee chair, Dr. Sunil Chirayath, for guidance, always being available and approachable, and all the assistance in all aspects of this research. He is an excellent academic, and a true gentleman.

I would like to thank my committee members, Dr. Pavel Tsvetkov and Dr. Joseph Bracci for their guidance and support throughout the course of this research.

Thanks also go to my friends and colleagues and the Nuclear Engineering department faculty and staff for making my time at Texas A&M University a great experience.

Finally, thanks to my mother and father for their continuous encouragement, prayers, love, and also endless financial support.

CONTRIBUTORS AND FUNDING SOURCES

Contributors

This work was supervised by a thesis committee consisting of Professor Sunil Chirayath [advisor] and Professor Pavel Tsvetkov [committee member] of the Department of Nuclear Engineering [Home Department] and Professor Joseph Bracci [committee member] of the Department of Civil Engineering [Outside Department].

All other work conducted for the thesis was completed by the student independently.

Funding Sources

NOMENCLATURE

SNM	Special Nuclear Material
TNT	Tri-Nitro Toluene
FEA	Finite Element Analysis
STR	Structure
ASD	Adversary Sequence Diagram
EASI	Estimate of Adversary Sequence Interruption
CD	Charge Diameter
HE	High Explosive
LD	Liner Distance
WD	Warhead Diameter
OD	Outer Distance
RHT	Riedel-Hiermaier-Thoma
RC	Reinforced Concrete
EOS	Equation of State
CAD	Computer-Aided Design
L	Length
H	Height
W	Width
PPS	Physical Protection System
RFT	Response Force Time

TABLE OF CONTENTS

LIST OF FIGURES

LIST OF TABLES

1. INTRODUCTION

1.1 Background

Nuclear power plants are critical facilities that need to be protected, because attack or sabotage on a nuclear power plant can cause significant harmful effects on humans including the release of high levels of radioactivity as an example. There are well-known examples, which show hazardous effects on humans, of a nuclear accident in Chernobyl, Ukraine and Fukushima Daiichi, Japan. In addition, it could also be an avenue for adversaries to steal special nuclear material (SNM) such as uranium or plutonium to make nuclear explosive devices after attack or sabotage on a nuclear power plant. Therefore, it is important to predict the blast load or its impact correctly on the structures that can be used in a nuclear power plant, because terrorists can attack a nuclear power plant using direct explosions by TNT (Tri Nitro Toluene) or other explosive materials, bullets, or linear shaped charges.

In this study, a terrorist is supposed to design a shaped charge using TNT explosive material, and the terrorist tries to make a hole and passes into one of nuclear reactor facilities so that the terrorist can sabotage the facility further or SNM that are used to make nuclear weapon devices. A target is considered as the high strength reinforced concrete wall that is used for the nuclear facility building construction, and the terrorist shoots the TNT shaped charge to make a hole on the target from a distance of 50 meters.

A shaped charge is often made as a cylinder filled with an explosive material, a detonator at one end and a hollow cavity with a metallic conical liner at the other. Upon detonation of the explosive, the conical liner collapses into a metallic jet with a very high speed excess of several thousand meters per second. The last part of the jet has lower velocity. The jet may penetrate to large depths which is several times of the charge diameter (CD). The penetration is often given

in the charge diameters. The penetration of a shaped charge increases with the jet length and density and decreases with higher target density.[1] A drawing of a shaped charge is shown in Figure 1.
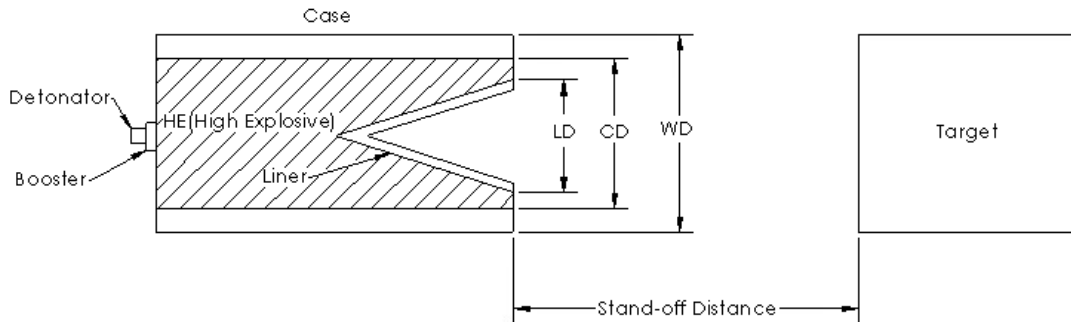
Figure 1. General 2D Drawing of Shaped Charge Design.

Where, the HE represents the high explosive material, the LD represents the liner distance, and the WD or OD represents the warhead diameter or the outer distance.

The shaped charge concept has been used and developed widely in various applications of military and civilian purpose. The main purpose of a shaped charge is to make a hole in a material that is otherwise difficult to penetrate through. Originally, shaped charges were first developed after World War I to penetrate tanks and other armored equipment.[3] However, further researches of the shaped charges in earnest were started after World War II for the military purpose. This is because shaped charges can efficiently damage tanks processing thick amour protection, bunkers and aircraft and are useful for attacking ships and submarines.[4] Although the research of the shaped charges have started to be developed for the military purpose, there are

2

various civilian applications which finds use in the peaceful purpose. Mining, a deep penetration

tunnel into the rock formation and oil well perforations are examples in civilian application.[5]

To conduct this study, ANSYS Simulation Software is used to predict the impact damage

and the penetration of a reinforced concrete wall target by a TNT shaped charge. ANSYS

simulation software is one of the strongest commercialized simulation software to solve

engineering problems or multi-physics' events such as electronics, fluids, impact and drop

testing, and high explosion analysis etc. Two different types of simulation software are coupled

for further advanced analysis within ANSYS Simulation Software. One is ANSYS Explicit

Dynamic STR (Structure) software and the other one is ANSYS AUTODYN software. ANSYS

Explicit Dynamic STR code provides suitable solutions of nonlinear dynamic events for a short

duration, including a drop and impact testing with low velocity or high velocity, deformation by

high pressure, explosion, and failure analysis etc. ANSYS AUTODYN code also provides

suitable solutions of nonlinear dynamic events similar to ANSYS Explicit Dynamic STR code,

but this software is focused on complicated nonlinear dynamic events like high explosions and

detailed damage responses of materials such as crack and fragment.

There are difficulties in this study to validate numerical results with existing experimental

data unless an experiment is performed for such evaluations. Therefore, several benchmark

simulations, which compare numerical results to the experimental data related to this study, are

studied and conducted before the simulations of this study are performed so that numerical

results of this study can be reasonable to the real scenarios. There are three major steps, with

assumptions, to conduct the numerical simulation. The first step is to simulate shaped charges

using ANSYS AUTODYN code to find the jet velocity of the liner fragment and to estimate the

size of the liner fragment created by the shaped charge design. From the data collected in

ANSYS AUTODYN code, the next step is to model a reinforced concrete wall and model the fragment by applying for necessary initial conditions and boundary conditions such as Fixed Support at all outer surface of the reinforced concrete wall model, Standard Earth Gravity for both of the reinforced concrete wall model and the fragment, and the velocity of the fragment to analyze the given problem using ANSYS Explicit Dynamic STR. The last step is to transfer the data modeled from ANSYS Explicit Dynamic STR code to ANSYS AUTODYN code to check the approximate hole size created by the shaped charge design.

1.2 Previous Work

Previous work on the simulation of various shaped charge designs, or various simulations of the jet penetration impact into steel based armor, plane concrete, or reinforced concrete has been a topic of discussion for decades. In 2009, Werner Riedel wrote a chapter titled, "10 Years RHT: A Review of Concrete Modeling and Hydrocode Applications" with the name of book titled "Predictive Modeling of Dynamic Process, pp 143-165".[8] The paper discusses the RHT (Riedel-Hiermaier-Thoma) concrete model that has proven in a number of worldwide applications to successfully link low dynamic strength details to shock physics and to be applicable across the dynamic range of numerical simulations.[8] The paper also discusses many dynamic load cases such as projectile and shaped charge penetration, contact detonation, internal and external blast loading that have been proven and validated through numerical codes for several decades, however the paper emphasizes that high training in numerical dynamic load field is significant to provide real life solutions efficiently.[8]

In 2014, Kamal Guendouz et al. published a paper titled, "Autodyn 2D Simulation of Shaped Charge Jet Formation and Penetration Mechanism into Multi-Layered Shielded Target".[9] The paper discusses the shaped charge jet formation depends on different parameters which has

4

effect on jet behavior such as jet velocity, breakup and penetration. Jet radius or liner thickness, shell thickness, liner material density, α angle and stand-off distance are evaluated for the purpose of investigating the effect on performance of shaped charge jet velocity and jet breakup phenomena. The paper discusses the effect of stand-off distance on shaped charge jet penetration into steel target.[9] The paper also discusses the efficiency of resulted numerical solutions by comparing with the experiments done and reported in literature and Brikhoff's theory which states any spherically symmetric solution of vacuum field equations must be static and asymptotically flat.[9,10]

In addition, in 2014, KRÁLIK Juraj published a paper titled, "Safety of Nuclear Power Plants against the Aircraft Attack".[11] The paper discusses the nonlinear dynamic analysis of the reinforced concrete building of nuclear power plant to the aircraft impact, and the paper discusses the calculation of dynamic response and damage evaluation of the reinforced concrete wall or place using the transient nonlinear analysis solution method in ANSYS.[11]

In 2017, Ezzedin Gauluta et al. published a paper titled, "Numerical Simulation of RC Panels Subjected to High Speed Projectile – Erosion Selection in AUTODYN-3D code".[8] The paper discusses the erosion effect on the numerical simulation of reinforced concrete (RC) panels subjected to the impact of high speed projectile (0.50 cal. Bullet). Also, the paper discusses the response of the bullet residual velocity and damage depth at front and rear faces of the concrete panel from variations of erosion strain values and mesh size of the concrete panel.[12]

1.3 Goals of Thesis

This project will be completed as follows:

1. Conduct literature search and benchmark simulations of shaped charge impact on concrete or steel.

2. Model a reinforced concrete wall and a high jet velocity fragment.

3. Conduct linear impact and penetration analysis on the reinforced concrete wall.

4. Conduct parametric studies to make a big enough size of the hole on the reinforce concrete wall for a person to pass through at a time.

5. Predict a big enough size of the hole created by a TNT shaped charge design so that a person can pass through the hole at a time.

6. Perform probability of interruption of adversary attack calculation by considering the vulnerability of physical protection system (PPS) at a nuclear facility if a shaped charge is used.

1.4 Significance

The goal of this thesis is to predict a big enough hole-size on a reinforced concrete wall by a TNT shaped charge design using a numerical simulation software under a scenario that a terrorist attacks or sabotages one of the nuclear facilities. Potentially, nuclear power plants can cause very harmful effects on humans including the release of high radioactivity if there are any accidents or a terrorist attacks. Shaped charges have started to be developed in the military purpose, also the shaped charges can be used in various applications for both military and civilian purpose. Thus, shaped charges can be one of the possible threats to be considered from a terrorist. However, the possible threats to the nuclear power plants, like destroying nuclear power plant facilities further, or stealing SNM that can be used to make a nuclear weapon device after the terrorist passes through the hole created, can be predicted and prevented in nuclear security area. In addition, this study can aim to provide better suggestions while contributing to the missions of nuclear nonproliferation and nuclear security.

2. NUMERICAL SIMULATION

2.1 Material Properties, Formulas, and Solvers

All material properties and EOS (Equation of State) were obtained from ANSYS AUTODYN Materials Library. Air, TNT, AL 2024-T4, Copper, Concrete 140 MPa, and Steel 4340 were used for the numerical modeling and simulation. Other settings or parameters that are not mentioned here were set with default values or none by ANSYS AUTODYN code. In solvers, Lagrange processor was applied for modeling solid continua and structures, and Euler processor was applied with multi-material flow for modeling fluids, gases, and large distortion.[13] Also, Erosion and Failure were applied to see a distortion phenomenon in Lagrange models. The materials of Air, TNT, AL 2024, Copper were used in modeling and simulating in Euler processor, and the materials of Copper, Concrete 140 MPa, and Steel 4340 were used in modeling and simulating in Lagrange processor.

Air has EOS of Ideal Gas with its material properties shown in Eq. 1 and Table 1 respectively.[13]

$$p = (\gamma - 1)\rho e + P_{shift} \qquad (1)$$

Where, γ is the adiabatic exponent, ρ is the density of air, e is internal air energy, and P_{shift} is a small initial pressure defined to give a zero starting pressure.

Table 1. Material Properties of Air.

Air	
Reference density (g/cm^3)	1.225e-3
EOS	Ideal gas
Gamma	1.400
Adiabatic constant	0.000
Pressure shift	0.000
Reference temperature (K)	288.200012
Specific heat (J/kg K)	717.599976

TNT has EOS of JWL (Jones, Wilkins and Lee) shown in Eq 2 which describes the detonation product expansion down to a pressure of 1 kbar for high energy materials and has been proposed by Jones, Wilkins and Lee[13]. Its material properties are shown in Table 2.

$$P = A\left(1 - \frac{w}{R_1 V}\right)e^{-R_1 V} + B\left(1 - \frac{w}{R_2 V}\right)e^{-R_2 V} + \frac{wE}{V} \qquad (2)$$

Where, the values of the constants A, B, R$_1$, R, w for many common explosives have been determined from dynamic experiments and are available in ANSYS AUTODYN material library.

Table 2. Material Properties of TNT.

TNT	
Reference density (g/cm^3)	1.630
EOS	JWL
Parameter A (kPa)	3.737700e+8
Parameter B (kPa)	3.747100e+6
Parameter R1	4.150
Parameter R2	0.900
Parameter w	0.350
C-J Detonation velocity (m/s)	6.930e+3
C-J Energy / unit volume (kJ/m^3)	6.000e+6
C-J Pressure (kPa)	2.100e+7

AL 2004-T4 and Copper has EOS of Shock, and its material properties are shown in Table 3, Table 4, and Table 5 respectively.[13]

Table 3. Material Properties of AL 2024-T4.

AL 2024-T4	
Reference density (g/cm^3)	8.900
EOS	Shock
Gruneisen coefficient	2.000
Parameter C1 (m/s)	5.328e+3
Parameter S1	1.338
Reference temperature (K)	300
Specific heat (J/kgK)	863.000061
Strength	Steinberg Guinan
Shear modulus (kPa)	2.860e+7
Yield stress (kPa)	2.600e+5
Maximum yield stress (kPa)	7.600e+5
Hardening constant	310.000
Hardening exponent	0.185
Melting temperature (K)	1.220e+3
Failure	None
Erosion	None

Table 4. Material Properties of Copper in Euler Processor.

Copper	
Reference density (g/cm^3)	8.900
EOS	Shock
Gruneisen coefficient	2.000
Parameter C1 (m/s)	3.940e+3
Parameter S1	1.489
Strength	None
Failure	None
Erosion	None

Table 5. Material Properties of Copper in Lagrange Processor.

Copper	
Reference density (g/cm^3)	8.900
EOS	Shock
Gruneisen coefficient	2.000
Parameter C1 (m/s)	3.940e+3
Parameter S1	1.489
Reference temperature (K)	295.149994
Specific heat (J/kgK)	0.386
Strength	Multilinear hardening
Shear modulus (kPa)	4.640e+7
Hardening	Isotropic
Failure	None
Erosion	Geometric strain
Erosion strain	0.0022
Type of geometric strain	Instantaneous

140 MPa Concrete has EOS of Alpha Porosity Plastic shown in Eq 3, also 140 MPa

Concrete has RHA (Riedel-Hiermaier-Thoma) model shown in Eq 4.[13]

$$\alpha = 1 + (\alpha_p - 1) \left(\frac{P_s - P}{P_s - P_e} \right)^n \tag{3}$$

Where, P_s is the solid compaction pressure at full compaction, P_e is the initial compaction

pressure at α_p, and e is the compaction exponent.

$$Y_{TXC} = f'_c \left[A_{FAIL} \left(P^* P^*_{spall} F_{RATE} \right)^{N_{FAIL}} \right] \tag{4}$$

Where, Y_{TXC} is the fracture surface, f'_c is the cylindrical strength, A_{FAIL}, N_{FAIL} are user defined

parameters, P^* is pressure normalized with respect to f'_c, P^*_{spall} is the normalized hydrodynamic

tensile limit, F_{Rate} is a rate dependent enhancement factor shown Eq 5, and its material

properties are shown in Table 6.[13]

$$F_{Rate} = \begin{cases} 1 + \left(\dfrac{\dot{\varepsilon}}{\dot{\varepsilon_0}}\right)^{\alpha} & \text{for P} > 1/3 f_c \text{ with } \dot{\varepsilon_0} = 30 \text{ x } 10^{-6} \text{ s}^{-1} \text{ (compression)} \\ 1 + \left(\dfrac{\dot{\varepsilon}}{\dot{\varepsilon_0}}\right)^{\delta} & \text{for P} < 1/3 f_c \text{ with with } \dot{\varepsilon_0} = 3 \text{ x } 10^{-6} \text{ s}^{-1} \text{(tension)} \end{cases} \quad (5)$$

Where, α is the compressive strain rate exponent and δ is the tensile strain rate exponent.

Table 6. Material Properties of 140 MPa Concrete.

140 MPa Concrete	
Reference density (g/cm^3)	2.750
EOS	P alpha
Bulk Modulus A1 (kPa)	3.527e+7
Strength	RHT Concrete
Shear Modulus (kPa)	2.206e+7
Compressive Strength, f_c (kPa)	1.400e+7
Failure	RHT Concrete
Damage Constant, D1	0.040
Damage Constant, D2	1.000
Tensile Failure	Hydro (Pmin)
Erosion	Geometric strain
Erosion strain	0.500
Type of geometric strain	Instantaneous

Steel 4340 has Johnson and Cook model which represents the strength behavior of materials, typically metals, subjected to large strains, high strain rates and high temperatures shown in Eq 4.[13]

$$\sigma_y = (A + B\varepsilon_p^n)(1 + Cln\dot{\varepsilon}_p)(1 - T_H^m) \quad (6)$$

Where, ε_p is the effective plastic strain, $\dot{\varepsilon}_p$ is the normalized effective plastic strain, T_H is the homogeneous temperature, and the material constants are A, B, C, n, and m. T_H is depended on the room temperature T_{room} and meeting temperature $T_{melting}$, and given by Eq 5, and Its material properties are shown in Table 7.[13]

11

$$T_H = \frac{T - T_{room}}{T_{melt} - T_{room}} \tag{7}$$

The Constants A, B C, n, m where A is the initial yield stress, B is the hardening constant, n is

the hardening exponent, C is the strain rate constant, and m is the thermal softening exponent.

Table 7. Material Properties of Steel 4340.

Steel 4340	
Reference density (g/cm^3)	7.83
EOS	Linear
Bulk modulus (kPa)	1.590e+8
Reference temperature (K)	295.149994
Specific heat (J/kgK)	477
Strength	Johnson Cook
Shear modulus (kPa)	8.18e+7
Yield stress (kPa)	7.92e+5
Hardening constant (kPa)	5.10e+5
Hardening exponent	0.26
Strain rate constant	0.014
Thermal softening exponent	1.03
Melting temperature (K)	1.793e+3
Ref. strain rate (s^{-1})	1.000
Failure	Principal strain
Principal tensile failure strain	0.002
Erosion	Geometric strain
Erosion strain	2.0000
Type of geometric strain	Instantaneous

2.2 Study of Simulation Codes and Benchmark Simulations

Before the numerical simulations of this study were performed, several benchmark studies were conducted using literature search, ANSYS tutorials, and published papers. First, the published paper titled "Autodyn 2D Simulation of Shaped Charge Jet Formation and Penetration Mechanism into Multi-Layered Shielded Target" by Kamal Guendouz et al. in 2014 was referred as the benchmark study for modeling and simulating TNT shaped charge.[9]

By Kamel Guendouz et al., a shaped charge was modeled using materials of AL 2024-T4 for the cylindrical case, TNT for the explosive material, and Copper for the metallic conical liner using ANSYS AUTODYN code. Then, the shaped charge modeled was simulated to investigate how deep into a steel target the shaped charge can penetrate within a steel target, which consists of Steel V250 material at different charge distances.

The benchmark simulation was performed to compare simulation results between the reference paper and the benchmark simulation. Before the simulation was performed in ANSYS AUTODYN code, 2D drawing was performed using AutoCAD (Computer-Aided Design) software to help visualize the model shown in Figure 2.
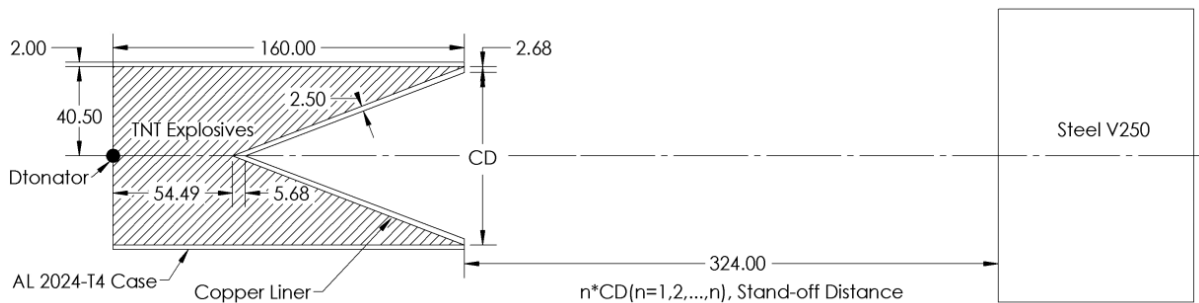
Figure 2. 2D Drawing for Benchmark Simulation (Dimensions are in mm).

Also, it could be used to calculate the mass of the explosive by the geometry of the volume of the cylinder (TNT) and cone (copper liner) with the known its materials' density, and the calculated TNT mass was 1.05 kg for the shaped charge modeled by the reference paper.

Here, the benchmark simulation shows only as an example that the steel target was located at a distance of 324 mm (4 CD) from the shaped charge. ANSYS AUTODYN input (left) and output (right) code for the benchmark simulation is shown in Figure 3.
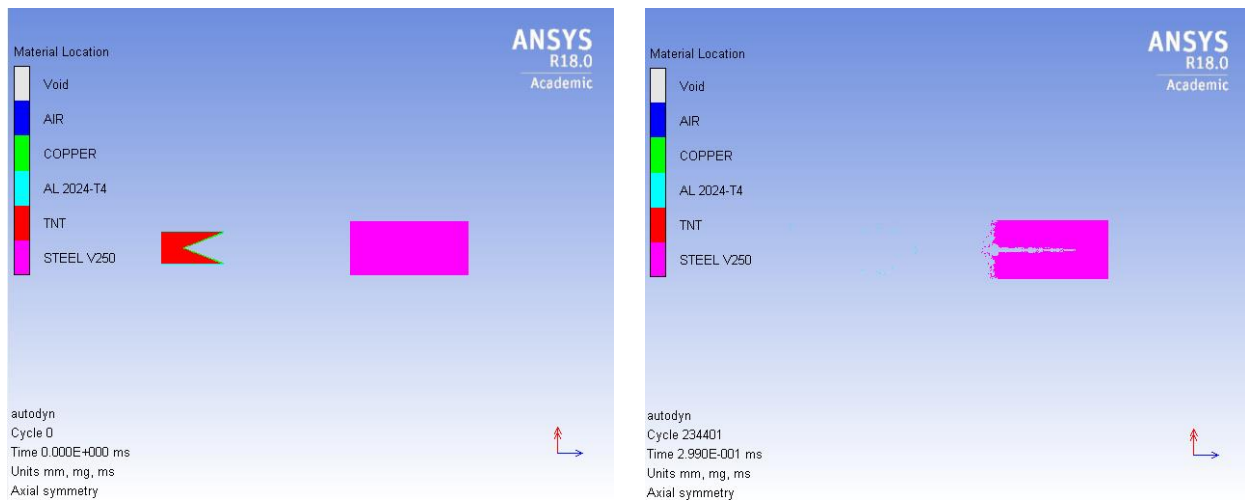
Figure 3. ANSYS AUTODYN Input and Output Code for Benchmark Simulation.

From the input and output code for the benchmark simulation, it resulted about 257 mm of the penetration depth in the steel target, and the result of the reference paper resulted 258.50 mm. Both of the results were not matched perfectly, because there were not available the full details of the simulation input data from the reference paper, however they agree reasonably well. Possible reasons of the difference could be the precision of the grid to measure the depth of penetration, solvers, or material data inputs of the steel target.

Second, the reinforced concrete was modeled through the literature search and ANSYS tutorials. Before beginning the study of numerical modeling, a reinforced concrete was drawn using AutoCAD software with dimensions of 1000 mm (L) x 200 mm (H) x 110 mm (W). This step was to aim the visibility for the modeling. The concrete wall was reinforced with 5 mm ø steel bars with spacing 50 mm in vertical direction. There was a space of 5 mm at the outermost steel bars. Also, there was a space of 27 mm at the outermost bottom steel bar. 2D drawing of the reinforced concrete and 2D drawing of details of the reinforced steel bars are shown in Figure 4 and Figure 5.
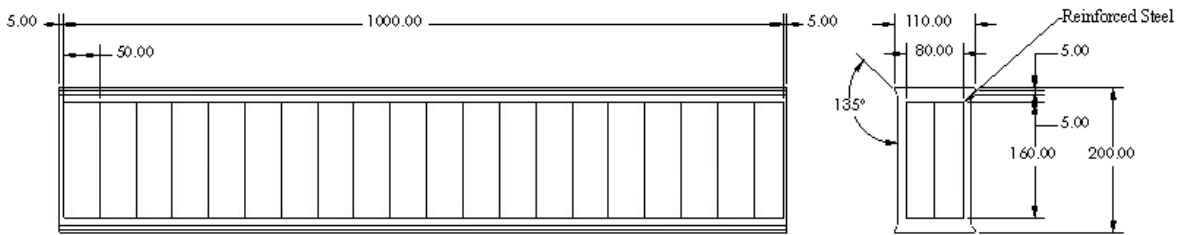
Figure 4. Study of Reinforced Concrete with Steel Bars in 2D Drawing (Dimensions are in mm).

Figure 5. Study of Reinforced Concrete of Steel Bars in 2D Drawing (Dimensions are in mm).

Afterwards, the reinforced concrete was modeled using ANSYS Explicit Dynamic STR code. In the code, the mesh size of 15 mm was applied to the 35 MPa concrete and the structure steel. Also, the conditions of the connection between the concrete and the steel bars were applied

as Frictionless and Reinforcement. The concrete with the reinforced steel bars in it and the

reinforced steel bars without the concrete are shown in Figure 6.

Figure 6. Study of Reinforced Concrete with Steel Bars in 3D Model.

Third, the published journal paper titled "Numerical Simulation of RC Panels Subjected

to High Speed Projectile – Erosion Selection in AUTODYN-3D code" by Ezzedin Gauluta et al.

in 2017 was referred as the benchmark study for the modeling and simulating the impact

investigation on the reinforced concrete model due to the TNT shaped charge in general.[12]

Lastly, the published paper titled "Experimental and numerical study on the flight and

penetration properties of explosively-formed projectile" by Wu J, Liu J, Du Y was referred to

assume the shape of the fragment (projectile) produced due to TNT shaped charge.[21] The paper

performed an actual experiment of TNT shaped charge on a steel target in order to compare

experimental results and numerical results. Also, the paper investigated the shape of the

explosively-formed projectile due to TNT shaped charge. In the paper, the shape of the projectile

was not a perfectly bullet shape, however it could be looked like a bullet shape reasonably. Thus, this paper assumed the shape of the fragment to be a bullet shape.

There were various methods to model a reinforced concrete model, and there were not enough details to know how the reference papers modeled a reinforced concrete. Also, the most of shaped charge simulations were done with a steel target by literature searching. Therefore, the benchmark simulation with a reinforced concrete target could not be performed, however material data inputs for the reinforced concrete could be referred from the paper[12] and idea of what configuration should be in a target materials by high velocity projectile such as bullets and shaped charges from the papers.[12,21]

2.3 Numerical Simulation Method and Results

The numerical simulation of this study was performed using a high speed computer

processor Intel Xeon E3-1505M v6 quad-core 3GHz, Nividia Quadro P5000, Intel HD Graphics

P630, and RAM 64GB DDR4 ECC. Also, ANSYS 18.0 Academic version was used in order to

perform the numerical simulation.

In this study, there were three major steps. The first step was to model a reinforced

concrete wall in ANSYS Explicit Dynamic STR code. The second step was to model and

simulate a TNT shaped charge in ANSYS AUTODYN code. The last step was to perform the

impact investigation on the reinforced concrete model due to TNT shaped charge in ANSYS

AUTODYN code. In the last step, there were two sub-steps. The first sub-step was to model the

fragment produced due to the TNT shaped charge with the reinforced concrete model in ANSYS

Explicit Dynamic STR code. The second sub-step was to transfer all modeled data from ANSYS

Explicit Dynamic STR code to ANSYS AUTODYN code to perform the impact investigation

simulation on the reinforced concrete model due to the TNT shaped charge in the last step.

Firstly, before beginning numerical modeling, a reinforced concrete wall as the target was

drawn using AutoCAD (Computer-Aided Design) software with dimensions of 1850 mm (L) x

1807 mm (H) x 300 mm (W). This step was to aim the visibility for the modeling. The concrete

wall was reinforced with 14 mm ø steel bars with spacing 100 mm in vertical direction and 160

mm in horizontal direction. There was a space of 20 mm at the outermost upper steel bar and the

outermost right and left steel bars. Also, there was a space of 27 mm at the outermost bottom

steel bar. 2D drawing of the reinforced concrete and 2D drawing of details of the reinforced steel

are shown in Figure 7 and Figure 8.

18
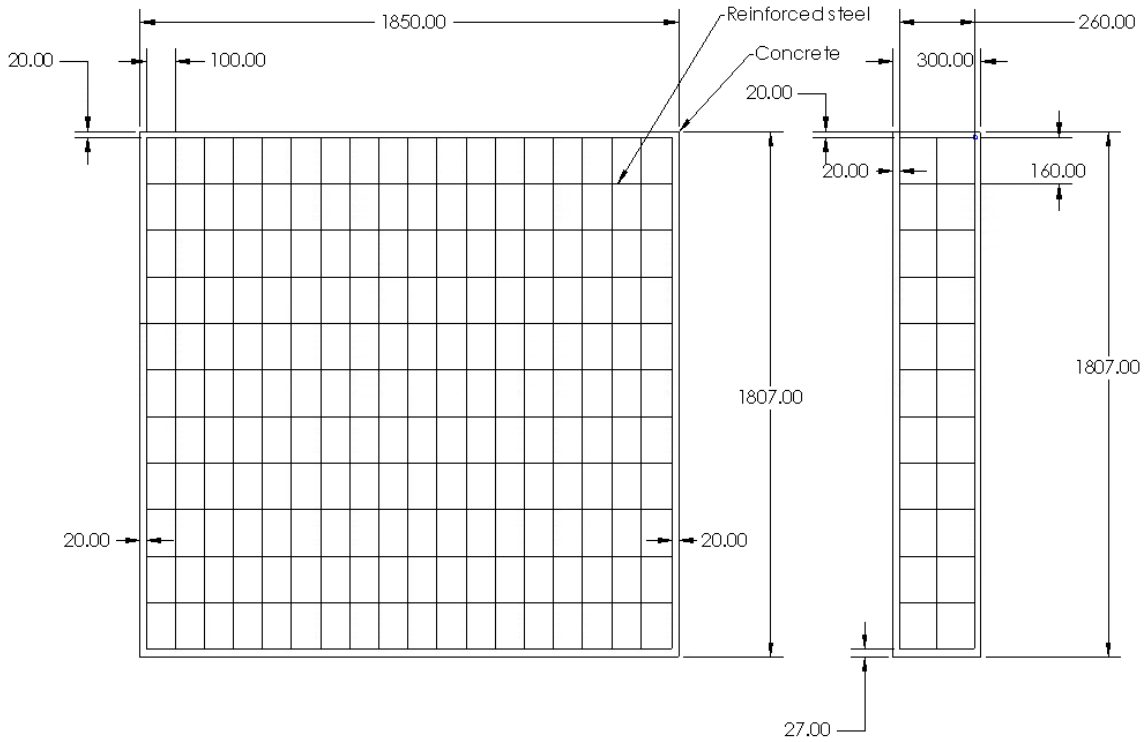
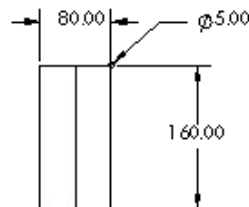Figure 7. 2D Drawing of Reinforced Concrete Wall (Dimensions are in mm).
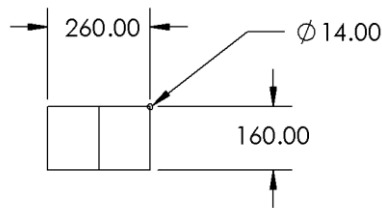
Figure 8. 2D Drawing of Reinforced Concrete Wall of Steel Bars (Dimensions are in mm).

Afterwards, the reinforced concrete was modeled using ANSYS Explicit Dynamic STR code. In the code, the mesh size of 22 mm was applied to the 140 MPa concrete and the steel 4030. Also, the conditions of the connection between the concrete and the steel bars were applied as Frictionless and Reinforcement. The concrete with the reinforced steel bars in it is shown in Figure 9, and the reinforced steel bars without the concrete are shown in Figure 10.
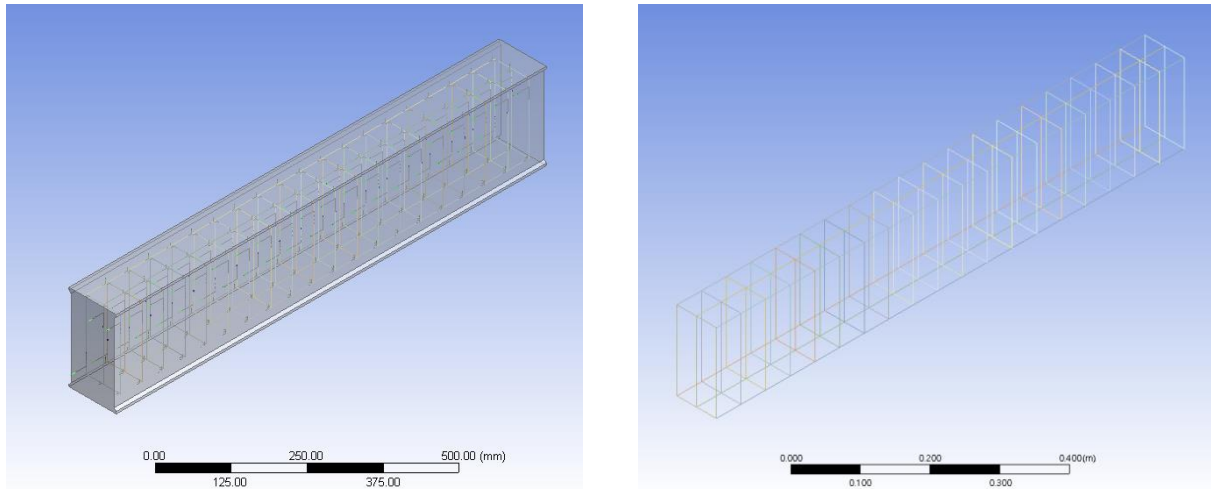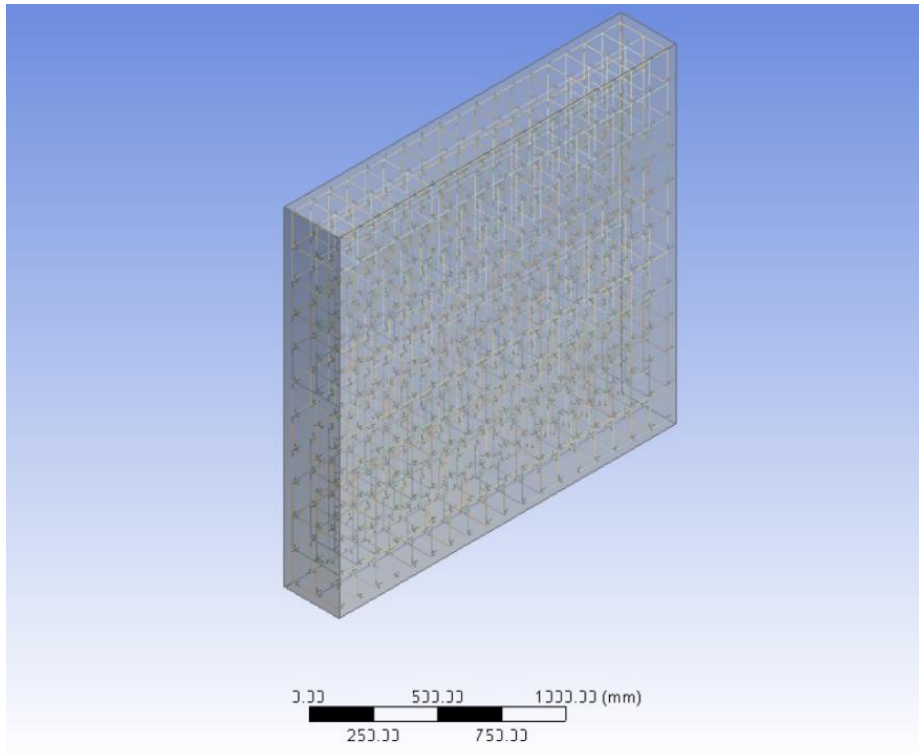
Figure 9. Reinforced Concrete Wall with Steel Bars in 3D Model.
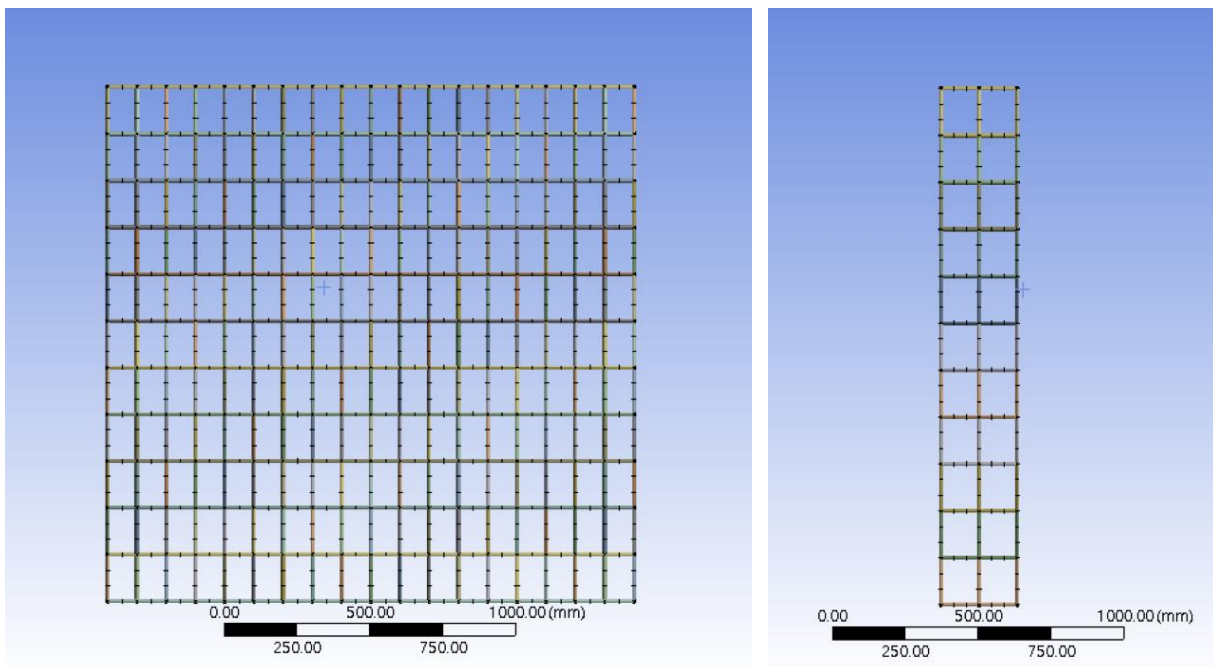
Figure 10. 3D Model of Steel Bars at Front and Side Views.

The reinforced concrete was modeled with materials of 140 MPa which had density of 2.75 g/cm^3 and 4030 steel which had density of 7.83 g/cm^3 obtained from ANSYS AUTODYN material library. The reinforced concreted model was considered with very high strength level of the concrete and the concrete was highly reinforced with steel bars. Therefore, to be more realistic, the strength level of the concrete considered were in the range of 20.68 - 48.26 MPa (3,000 - 7,000 psi) which could be typically used for reinforced concrete beams, slabs, columns and walls.[24]

Second, the numerical modeling and simulating of the TNT shaped charges were performed in ANSYS AUTODYN code. Before beginning, a design of shaped charge was drawn in 2D using AutoCAD software shown in Figure 11.
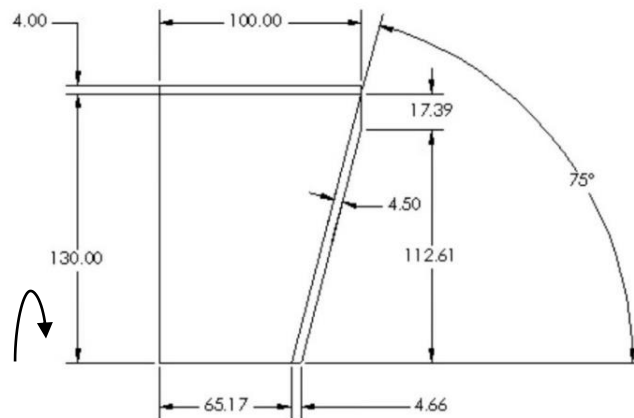
Figure 11. 2D Drawing of TNT Shaped Charge as Beginning Design
(Dimensions are in mm).

This step was performed, because the TNT shaped charges were modeled and simulated as 2D in ANSYS AUTODYN code, thus it helps to visualize the model. Also, this step was aimed to calculate the amount of TNT in designed models. The amount of TNT was calculated

21

by the geometry of the volume of the cylinder (TNT) and cone (copper liner) with the known materials' density. The first design of the TNT shaped charge model was calculated with the amount of 7.64 kg TNT.

Then, the TNT shaped charge was modeled and simulated in ANSYS AUTODYN code shown in Figure 12. Dense blue represents air, red represents TNT, light green represents aluminum 2024-T4 which is the outer cylindrical case for TNT, and light blue represents copper which is the conical shaped of the liner.
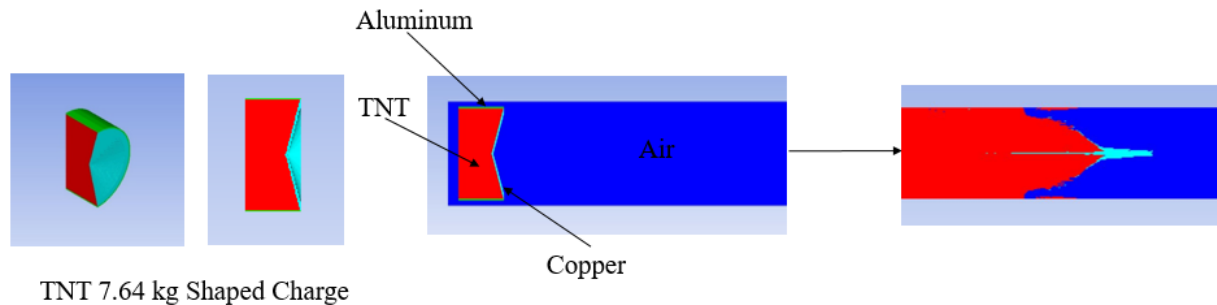
Figure 12. Numerical Modeling and Simulation of 7.64 kg TNT Shaped Charge.

In the numerical simulation, the mesh size of the shaped charge study was 1 mm, and the initial condition of Air that was the internal energy was applied as 2.068e+5 J/kg at 288 K.[19] Also, the flow-out boundary condition as the equilibrium state on all materials used was applied to the air, then the simulation was executed. The numerical model of the TNT shaped charge was designed and simulated in 2D, however the model could be represented in 3D by rotating x-axis of 360°.

The shape of the fragment produced due to the explosion of the TNT shaped charge was assumed similar to the bullet shape referring from the published paper.[10] Using the Axes in the Plot section of the View tap, the size was estimated measuring from the front tip to the end tip

22

for the length of the fragment and the diameter at the end tip for the diameter of the fragment shown in Figure 13.
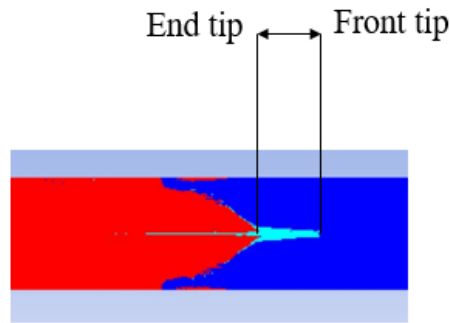
Figure 13. Fragment Measurement Point.

The data of the incident velocity where the fragment was turned right to be the bullet shape fully was resulted in the output. The velocity output was 2039.9 m/s, and the size of the fragment was measured 159 mm length from the front tip to the end tip and 38 mm diameter at the end of the tip.

Third, the fragment was modeled combining with the modeled reinforced concrete in ANSYS Explicit Dynamic STR code shown in Figure 14. In this modeling, the mesh size for the fragment was 22 mm which was same as the reinforced concrete modeling. Also, initial conditions and boundary conditions were applied to the model as Fixed Support at all outer surface of the reinforced concrete model, Standard Earth Gravity for both of the reinforced concrete model and the fragment, and the velocity of the fragment. For the velocity condition of the fragment, it was necessary to be applied as the initial conditions in the-negative-x direction, not as boundary conditions. This was because there is difference between the boundary condition and the initial condition. The initial condition is time dependence and the boundary condition is

space dependence. Also, the fragment was modeled at 2 -m away from the reinforced concrete

model, and the modeled reinforced concrete and fragment is shown in Figure 14.
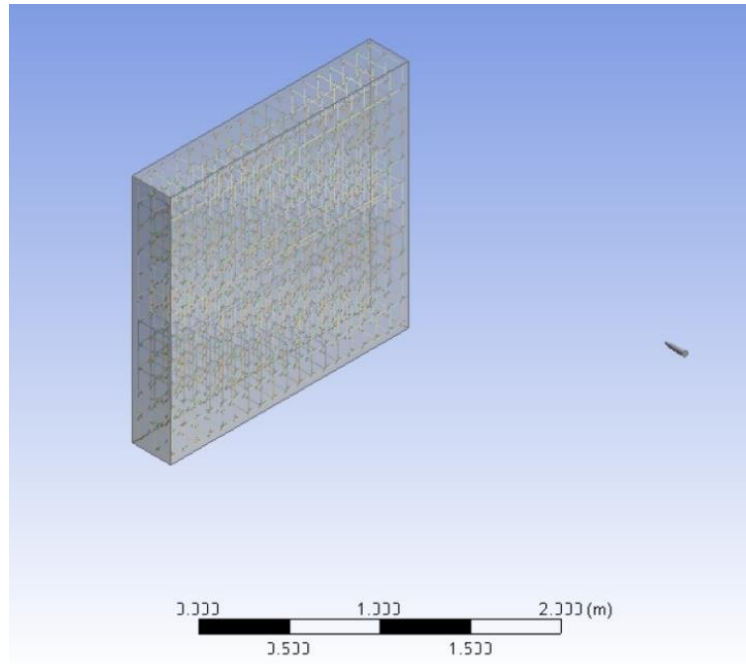
Figure 14. Reinforced Concrete Wall with Fragment due to 7.64 kg TNT Shaped Charge.

Lastly, the data of the modeled reinforced concrete and fragment were transferred to

ANSYS AUTODYN code from ANSYS Explicit Dynamic STR code in order to simulate the

entire model together at a distance of 50 -m between the reinforced concrete and the fragment.

When the modeled reinforced concrete and fragment were transferred to the ANSYS

AUTODYN code, the location of the fragment was not centered. Thus, the fragment was located

to be at centered and 50 -m away from the reinforced concrete model. The re-location step of the

fragment was conducted by steps following Setup→ Components→ Translate in

Transformations. The other settings remained with default values that were set up automatically

24

when the all designed models were transferred to ANSYS AUTODYN code. Then, all settings of

this numerical simulation method was completed for the impact investigation on the reinforced

concrete model due to the TNT shaped charge in ANSYS AUTODYN code shown in Figure 15.

In the final settings of the TNT shaped charge model, initially the fragment was located at 2 -m

away from the reinforced concrete, because the size of the fragment was not big enough to see at

the location of 50 -m away from the reinforced concrete.
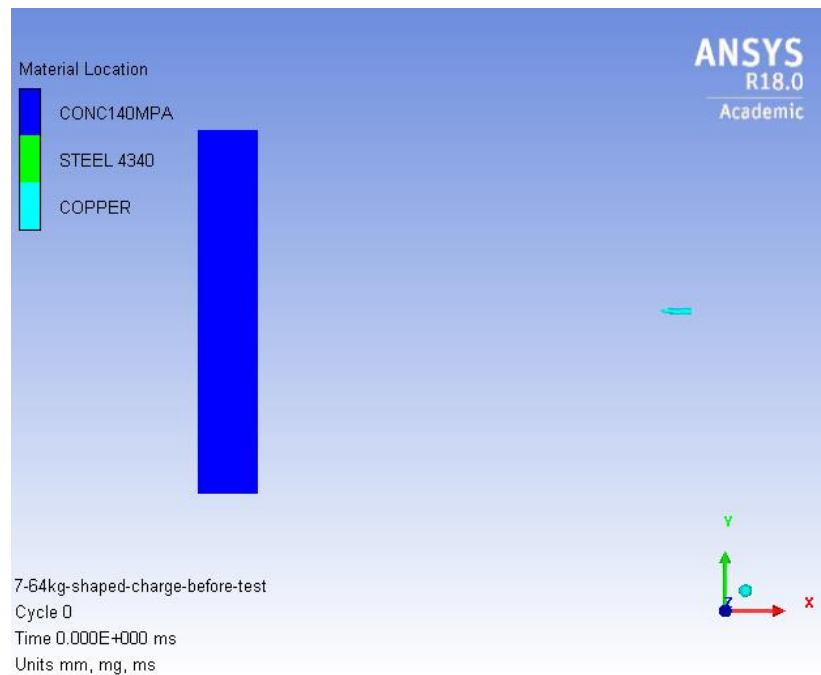
Figure 15. Final Simulation Settings of 7.64 kg TNT Shaped Charge.

After all settings were completed in ANSYS AUTODYN code, the simulation was

executed. The fragment produced due to 7.64 kg TNT shaped charge took 27.20 ms with the

incident velocity of 2039.9 m/s in order to create an impact on the reinforced concrete model.

The fragment was able to penetrate the reinforced concrete model fully, and it created a hole on

the reinforced concrete model. The hole size was measured in horizontal direction using the

Axes, and the hole size was 86 mm at the front side and 103 mm at the back side, and the result

of the simulation is shown in Figure 16 and Figure 17.
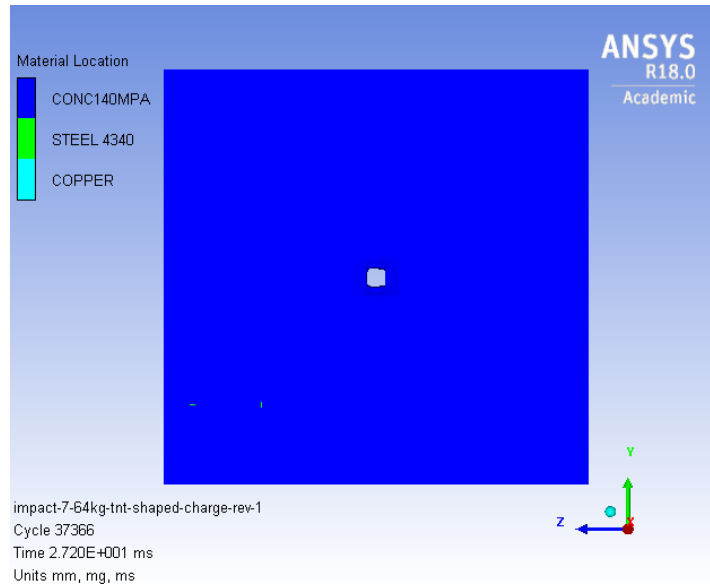
Figure 16. Hole Created at Front Side due to 7.64kg TNT Shaped Charge.
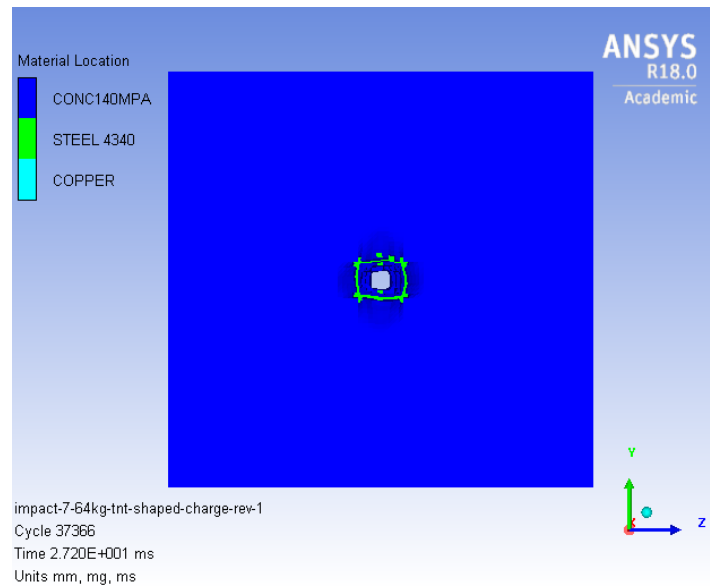
Figure 17. Hole Created at Back Side due to 7.64kg TNT Shaped Charge.

2.4 Parametric Studies and Results

After the numerical simulation was completed, parametric studies of TNT shaped charges

were conducted in order to investigate the creation of a big enough size of the hole on the

reinforced concrete model so that a person can pass through. This was because the hole size of

86 mm at the front side and 103 mm at the back side due to 7.64 kg TNT shaped charge were

created on the reinforced concrete model, but this was not enough size for a person to pass

through. Thus, for the parametric studies, the horizontal or vertical lengths, and the thickness of

liners were increased using the first designed 7.64 kg TNT shaped charge.

2.4.1 Parametric Study of Horizontal Length Increase

First, the parametric study of increasing horizontal lengths of TNT shaped charge was

conducted. There were three cases in this parametric study. The horizontal length for each case

was increased twice from the first TNT shaped charge design. 2D drawings were completed to

calculate amount of TNT and aim for modeling visually before the numerical simulation was

performed in ANSYS AUTODYN code. and the calculated amount of TNT for the parameter

study was 16.30 kg, 33.61 kg, and 59.57 kg shown in Figure 18, 19, and 20 respectively.
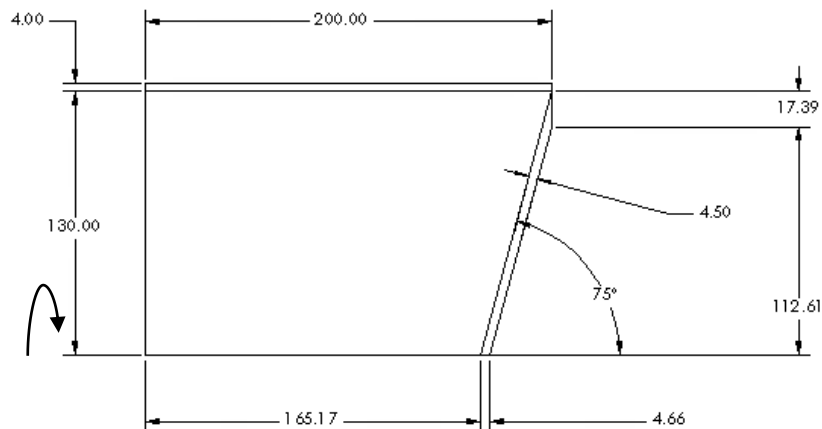
Figure 18. 2D Drawing of 16.30 kg TNT Shaped Charge (Dimensions are in mm).

27
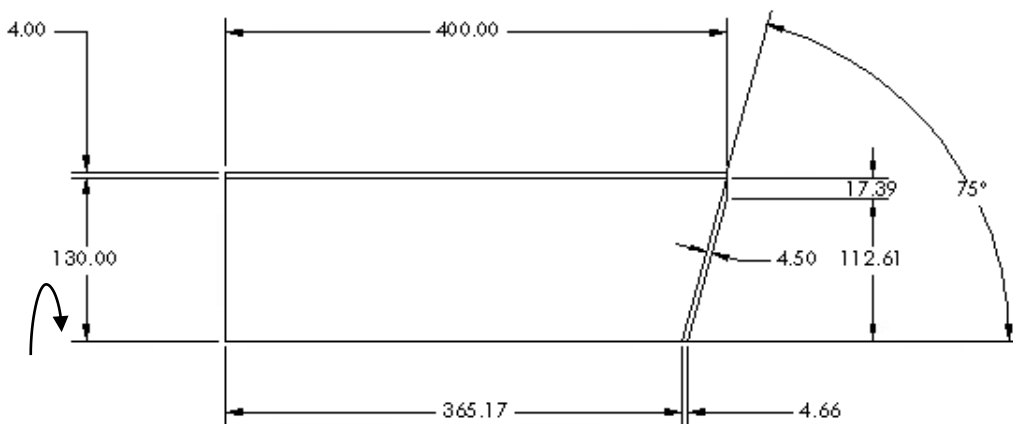
Figure 19. 2D Drawing of 33.61 kg TNT Shaped Charge (Dimensions are in mm).
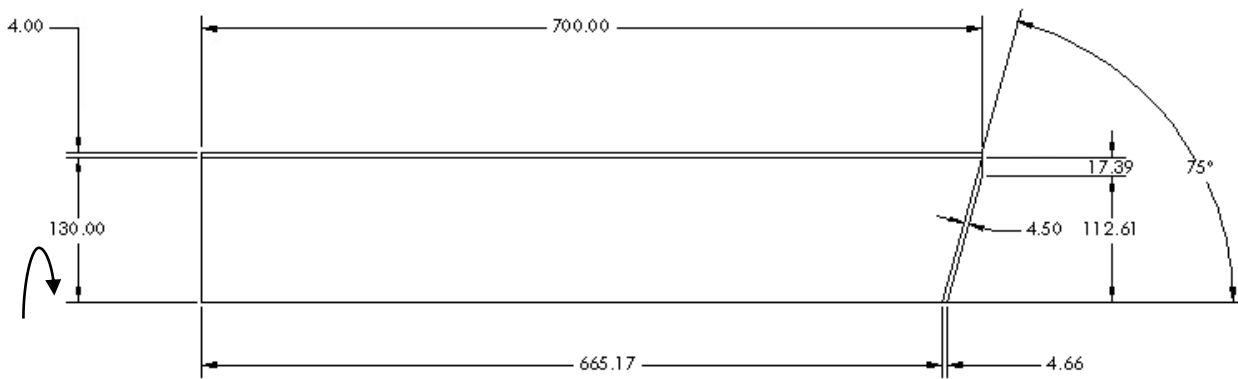
Figure 20. 2D Drawing of 59.57 kg TNT Shaped Charge (Dimensions are in mm).

Second, the increase of the horizontal length of the TNT shaped charges were modeled and simulated using ANSYS AUTODYN code in order to obtain the incident velocity output and the size of the fragment produced due to TNT shaped charge for each case shown in Figure 21.

TNT 16.30 kg Shaped Charge

TNT 33.61 kg Shaped Charge

TNT 59.57 kg Shaped Charge
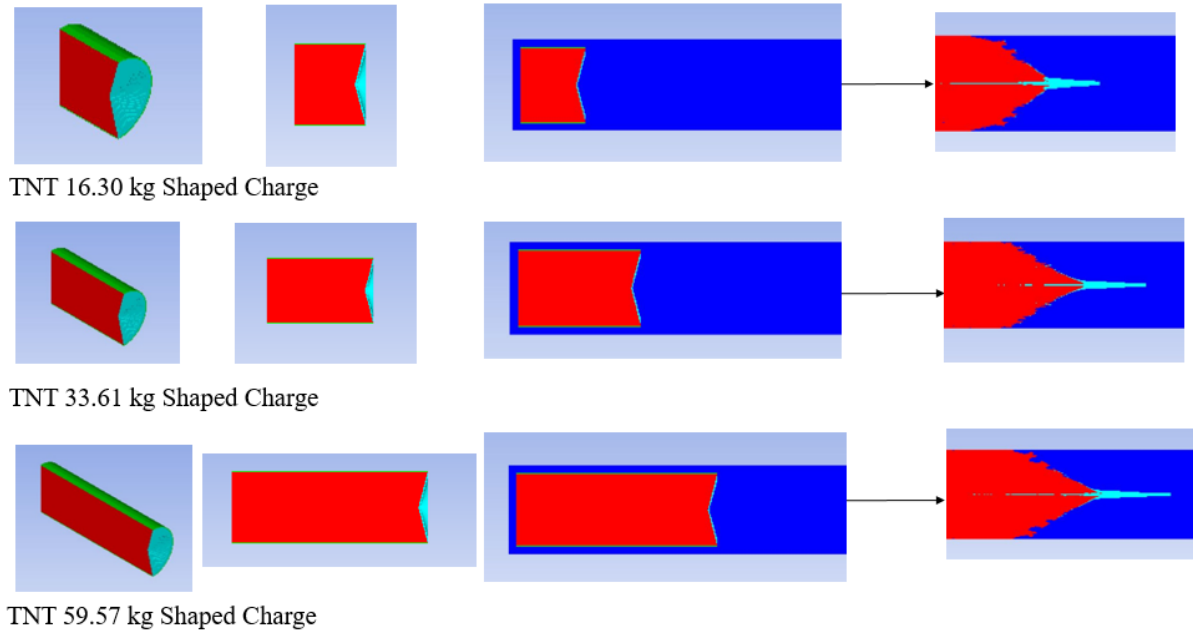
Figure 21. Parametric Studies of TNT Shaped Charges in Horizontal Length Increase.

After the simulation of the TNT shaped charges in the horizontal length increase was completed in ANSYS AUTODYN code, the incident velocity data output was obtained and the size of the fragment was measured the results obtained are shown in Table 8.

Table 8. TNT Shaped Charges' Results as Horizontal Length Increased.

Horizontal Length Increase (mm)	Shaped Charge TNT Amount (kg)	Incident Velocity (m/s)	Time of Incident Velocity (ms)	Estimated Size of Fragment (mm)
100	7.64	2039.9	0.18937	Length: 159, Ø: 19
200	16.30	2412.0	0.20870	Length: 173, Ø: 19
300	33.61	2758.3	0.40264	Length: 185, Ø: 19
700	59.57	2975.4	0.50017	Length: 248, Ø: 19

The resulted incident velocity data was plotted versus the TNT amount as the horizontal length increased shown in Figure 22.
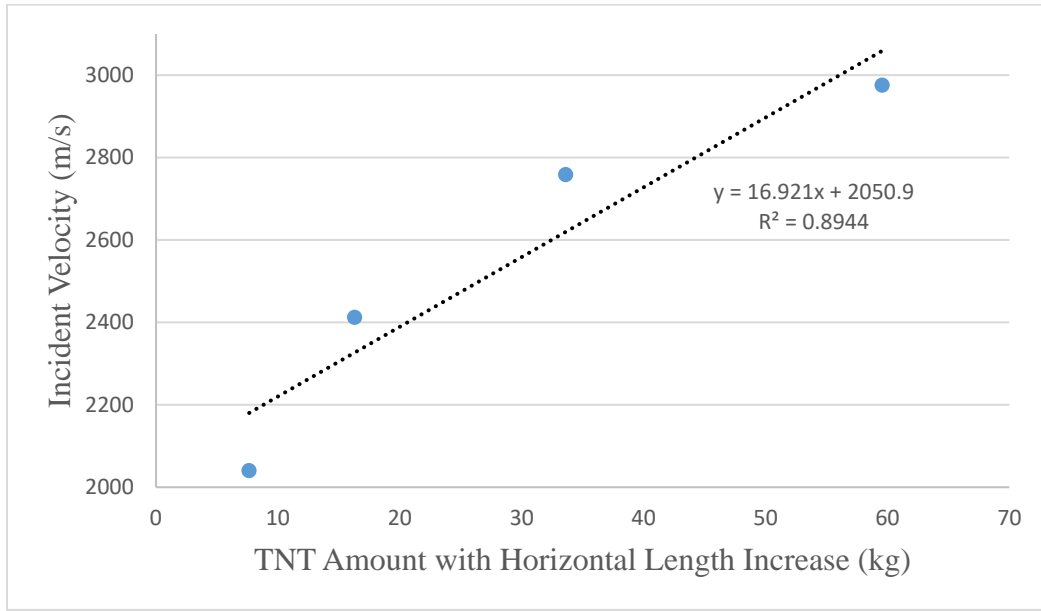
Figure 22. Incident Velocity versus TNT Amount Plot as Horizontal Length Increased with Linear Line Fitting.

Figure 22 shows the linear relationship between the incident velocity of the shaped charge and corresponding TNT mass. Considering the value of correlation coefficient, $R^2 = 0.8944$, the fitting shows a good linear relationship. Thus, the incident velocity of the shaped charge increases as the mass of TNT with the horizontal length increases.

After the TNT shaped charge simulation for each case was completed in ANSYS AUTODYN code, the fragment produced due to the TNT shaped charge was modeled with the reinforced concrete model in ANSYS Explicit Dynamic STR code shown in Figures 23, 24, and Figure 25. Then, the initial conditions and boundary conditions were applied in order to perform

the impact investigation simulation due to TNT shaped charge for each case on the reinforced

concrete model in ANSYS AUTODYN code.
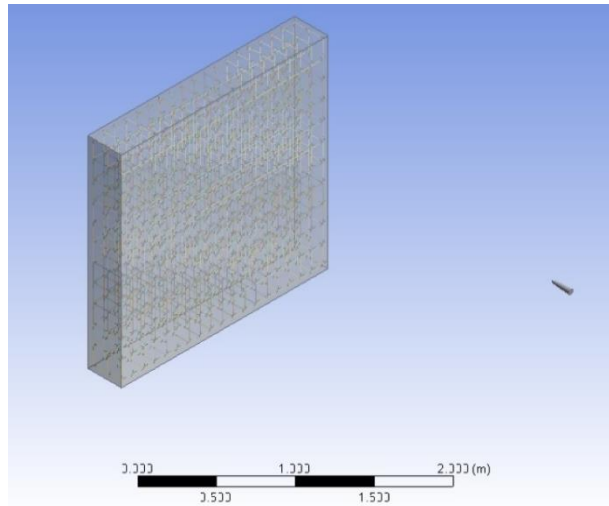
Figure 23. Reinforced Concrete Wall with Fragment due to 16.30 kg TNT Shaped Charge.
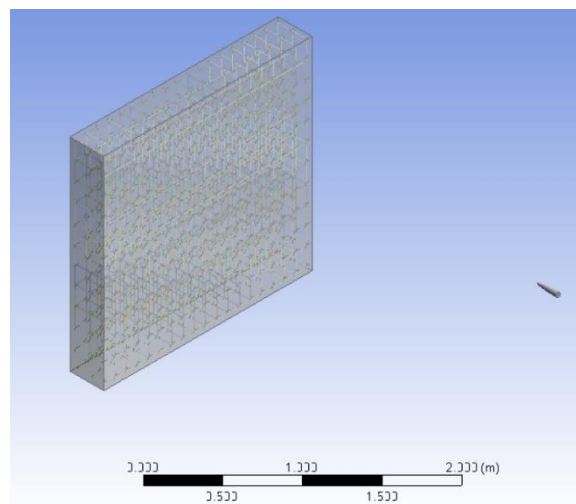
Figure 24. Reinforced Concrete Wall with Fragment due to 33.61 kg TNT Shaped Charge.
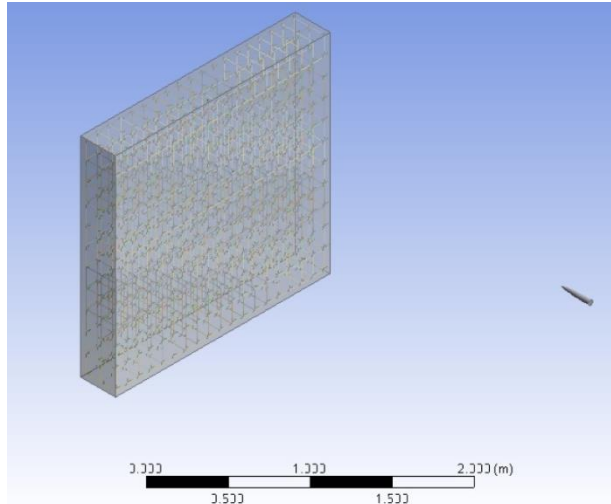
Figure 25. Reinforced Concrete Wall with Fragment due to 59.57 kg TNT Shaped Charge.

Lastly, the reinforce concrete modeled with the fragment for each case was transferred to ANSYS AUTODYN code from ANSY Explicit Dynamic STR code shown in Figures 26, 27, and Figure 28. The figures represent the final simulation settings of the impact investigation on the reinforced concrete due to TNT shaped charge in ANSYS AUTODYN code.
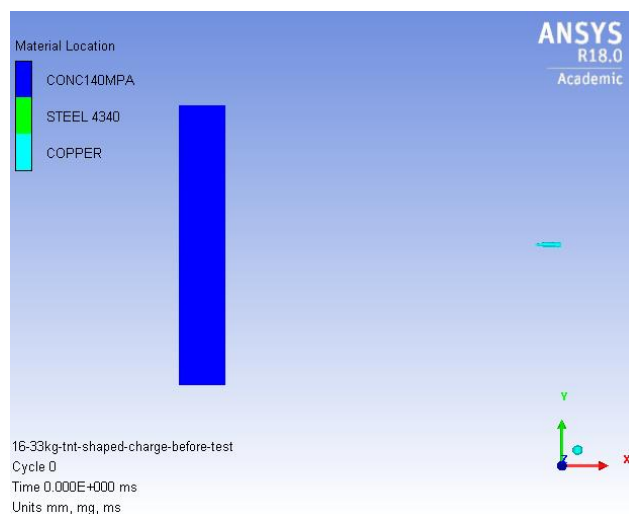
Figure 26. Final Simulation Settings of 16.30 kg TNT Shaped Charge.
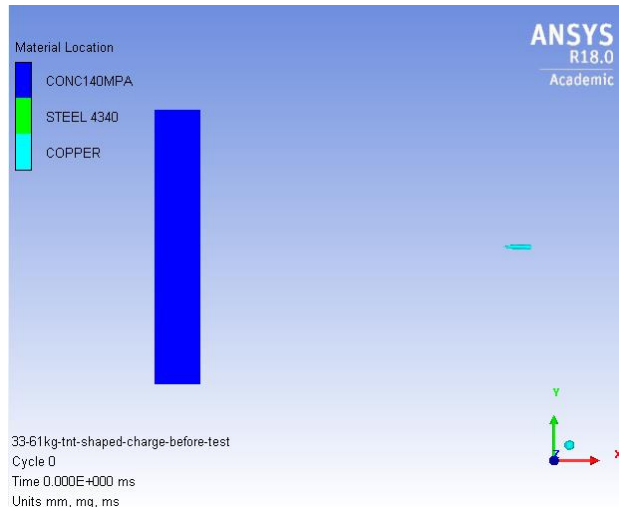
Figure 27. Final Simulation Settings of 33.61 kg TNT Shaped Charge.
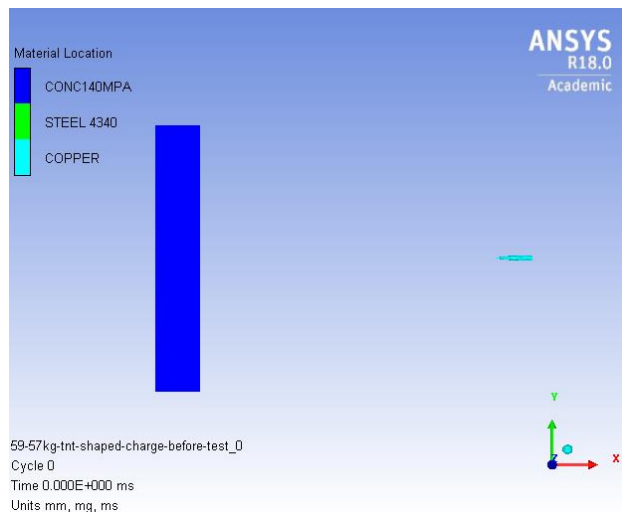
Figure 28. Final Simulation Settings of 59.57 kg TNT Shaped Charge.

After the final settings of the simulation was completed in ANSYS AUTODYN code, the fragment produced due to 16.30 kg TNT shaped charge took 21.47 ms with the incident velocity of 2412.0 m/s in order to create an impact on the reinforced concrete model. The fragment was able to penetrate the reinforced concrete model fully, and it created a hole on the reinforced

concrete model. The hole size was measured in horizontal direction using the Axes, and the hole

size was 87 mm at the front side and 105 mm at the back side shown in Figure 29 and Figure 30.
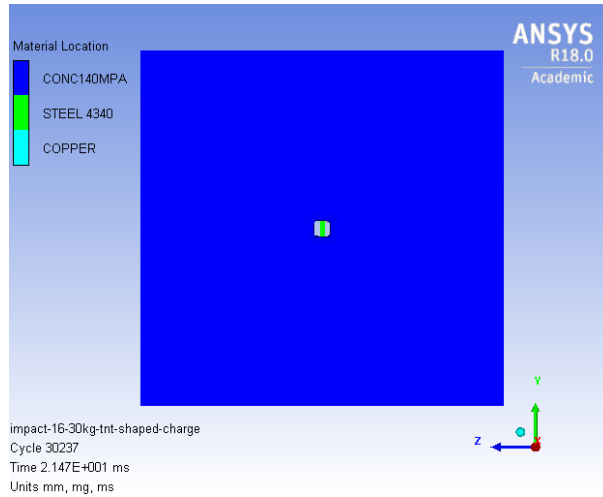
Figure 29. Hole Created at Front Side due to 16.30 kg TNT Shaped Charge.
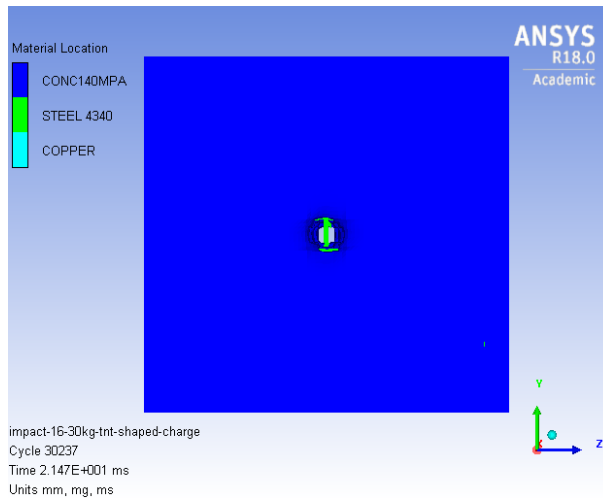
Figure 30. Hole Created at Back Side due to 16.30 kg TNT Shaped Charge.

The fragment produced due to 33.61 kg TNT shaped charge took 18.92 ms with the

incident velocity of 2758.3 m/s in order to create an impact on the reinforced concrete model.

The fragment was able to penetrate the reinforced concrete model fully, and it created a hole on the reinforced concrete model. The hole size was measured in horizontal direction using the Axes, and the hole size was 90 mm at the front side and 107 mm at the back side shown in Figure 31 and Figure 32.
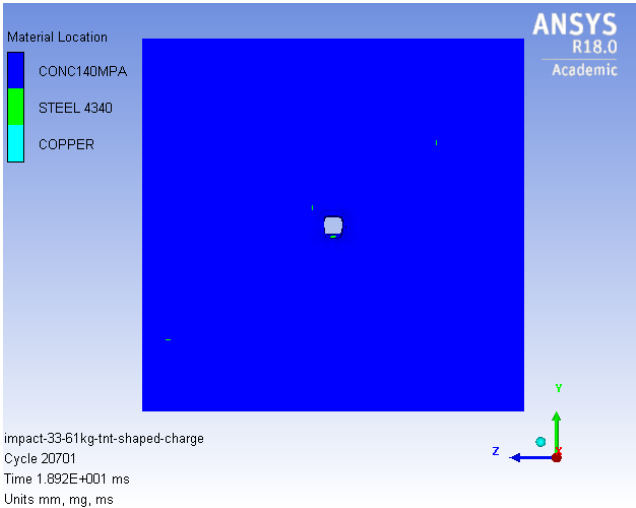
Figure 31. Hole Created at Front Side due to 33.61 kg TNT Shaped Charge.
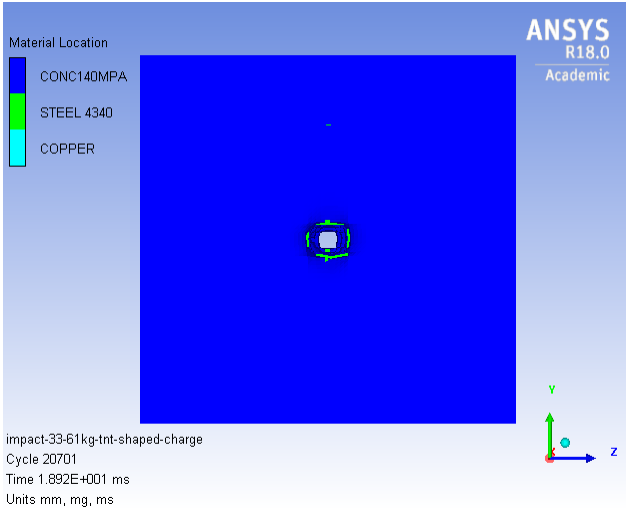
Figure 32. Hole Created at Back Side due to 33.61 kg TNT Shaped Charge.

The fragment produced due to 59.57 kg TNT shaped charge took 18.11 ms with the incident velocity of 2957.4 m/s in order to create an impact on the reinforced concrete model. The fragment was able to penetrate the reinforced concrete model fully, and it created a hole on the reinforced concrete model. The hole size was measured in horizontal direction using the Axes, and the hole size was 92 mm at the front side and 110 mm at the back side shown in Figure 33 and Figure 34.
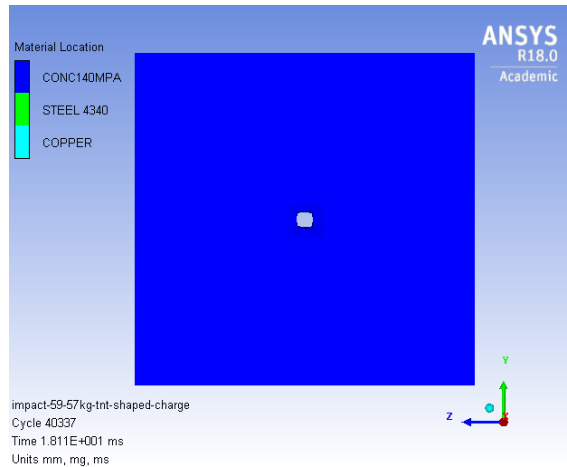
Figure 33. Hole Created at Front Side due to 59.57 kg TNT Shaped Charge.
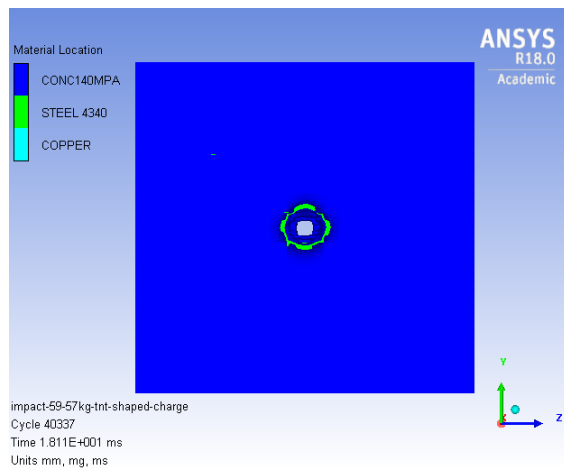
Figure 34. Hole Created at Back Side due to 59.57 kg TNT Shaped Charge.

From the parametric study of the horizontal length increase for each case, the diameter of the fragments were same, however the length of the fragments was increased. Also, the incident velocity of the fragments were increased. The size of holes were slightly increased as the horizontal length of TNT shaped charge was increased. The summary of the parametric studies of the horizontal length increase is shown in Table 9.

Table 9. Summary Results of Horizontal Length Increase.

Horizontal Length Increase (mm)	Shaped Charge TNT Amount (kg)	Incident Velocity (m/s)	Estimated Size of Fragment (mm)	Front Side Hole Size (mm)	Back Side Hole Size (mm)
200	16.30	2412.0	Length: 173, Ø: 19	87	105
300	33.61	2758.3	Length: 185,Ø: 19	90	107
700	59.57	2975.4	Length: 248, Ø: 19	92	110

2.4.2 Parametric Study of Vertical Length Increase

The parametric study of increasing vertical lengths of TNT shaped charge was conducted. There were three cases in this parameter study. The vertical length for each case was increased in order to match with TNT amount in the parameter study of the horizontal length increase. Firstly, 2D drawings were completed to calculate the amount of TNT and aim for modeling visually before the numerical simulation was performed in ANSYS AUTODYN code, and the calculated TNT amount for the parameter study was 15.35 kg, 28.86 kg, and 45.60 kg shown in Figures 35, 36, and Figure 37 respectively. The amount of TNT calculated in the parameter study of vertical length increase could not be exactly same as the TNT amount calculated in the parameter study of horizontal length increase because the amount of TNT was calculated by the geometry. However, both of the parameter studies had approximately similar TNT amounts.
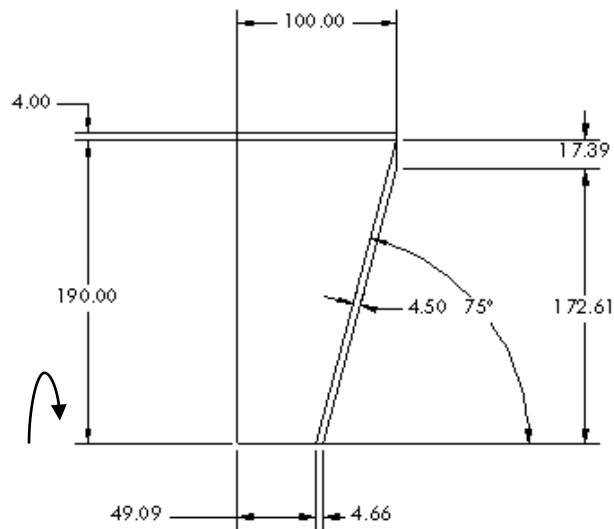
Figure 35. 2D Drawing of 15.35 kg TNT Shaped Charge (Dimensions are in mm).
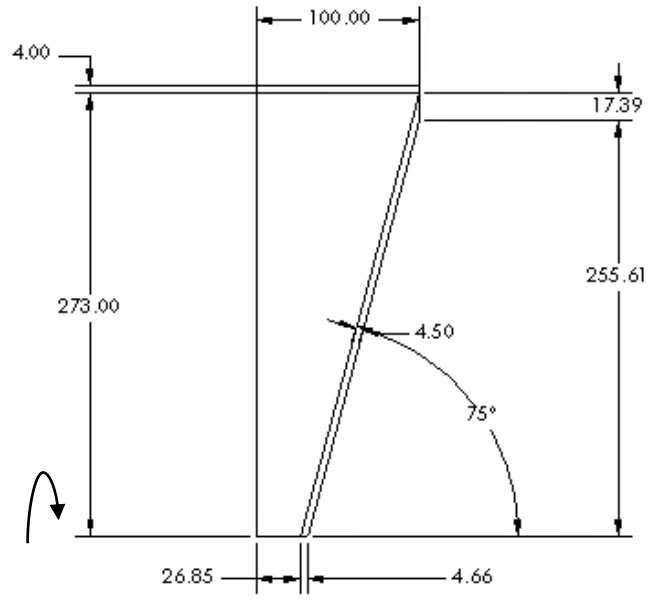
Figure 36. 2D Drawing of 28.86 kg TNT Shaped Charge (Dimensions are in mm).
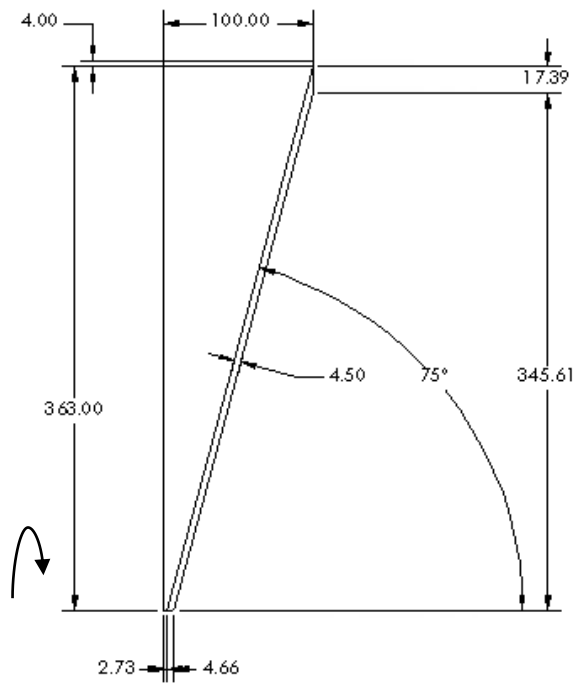
Figure 37. 2D Drawing of 45.60 kg TNT Shaped Charge (Dimensions are in mm).

Second, the increase of the vertical length of the TNT shaped charges were modeled and simulated using ANSYS AUTODYN code in order to obtain the incident velocity output and the size of the fragment produced due to the TNT shaped charge for each case shown in Figure 38.

TNT 15.35 kg Shaped Charge

TNT 28.86 kg Shaped Charge

TNT 45.60 kg Shaped Charge
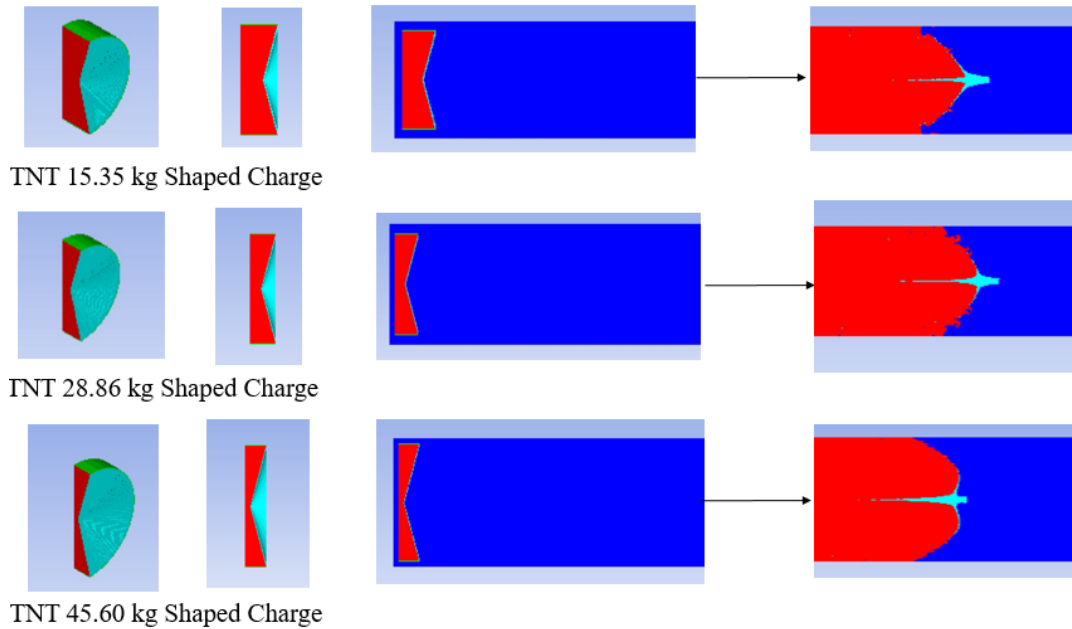
Figure 38. Parametric Studies of TNT Shaped Charges in Vertical Length Increase.

After the simulation of the TNT shaped charges in the vertical length increase was completed in ANSYS AUTODYN code, the incident velocity data output was obtained and the size of the fragment was measured by using axis shown in Table 10. However, 45.60 kg TNT shaped charge was not considered for the simulation of the impact investigation on the reinforced concrete in this case. This was because the shape of the fragment was assumed as the bullet shape, however the shape of the fragment in this case was not the bullet shape. Possible reason why the shape of the fragment produced by 45.60 kg TNT shaped charge could be different is that the vertical length was too long compared to its horizontal length. The gap between TNT

41

and the tip of corn of the copper liner was too short, thus the fragment wasn't able to be shaped

as bullet shape by 45.60 kg TNT shaped charge.

Table 10. TNT Shaped Charges' Results as Vertical Length Increased.

Vertical Length Increase (mm)	Shaped Charge TNT Amount (kg)	Incident Velocity (m/s)	Time of Incident Velocity (ms)	Estimated Size of Fragment (mm)
100	7.64	2039.9	0.18937	Length: 159, Ø: 19
190	15.35	2134.5	0.27829	Length: 104, Ø: 24
273	28.86	2159.6	0.40906	Length: 112, Ø: 29
363	45.60	2153.2	0.56105	Not Available

The incident velocity data resulted was plotted versus the TNT amount as the horizontal

length increased shown in Figure 39.
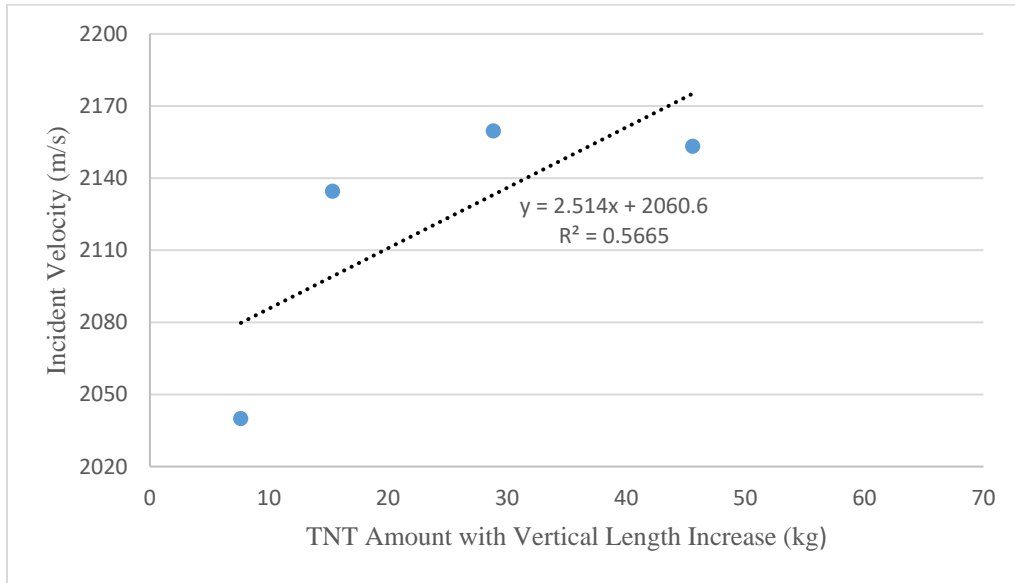
Figure 39. Incident Velocity versus TNT Amount Plot as Vertical Length Increased
with Linear Line Fitting.

Figure 39 shows the linear relationship between the incident velocity of the shaped charge and

corresponding TNT mass. Considering the value of correlation coefficient, $R^2 = 0.5665$, the

fitting is not highly within a good linear relationship. However, the value of correlation

coefficient, $R^2 = 0.9249$, shows a good polynomial relationship with the second order polynomial

equation shown in Figure 40.

43
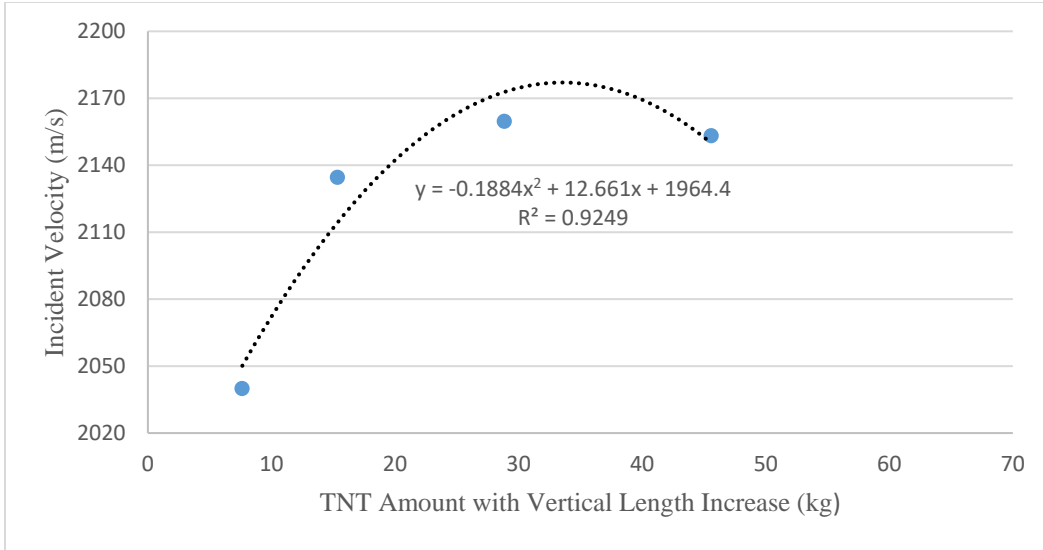
Figure 40. Incident Velocity versus TNT Amount Plot as Vertical length Increased with Polynomial Fitting.

Therefore, the incident velocity of the shaped charge is not considered to be increasing or decreasing as the mass of TNT with the vertical length increases.

After the TNT shaped charge simulation for each case was completed in ANSYS AUTODYN code, the fragment produced due to the TNT shaped charge was modeled with the reinforced concrete model in ANSYS Explicit Dynamic STR code shown in Figure 41 and Figure 42. Then, the initial conditions and boundary conditions were applied in order to perform the impact investigation simulation due to TNT shaped charge for each case on the reinforced concrete model in ANSYS AUTODYN code.
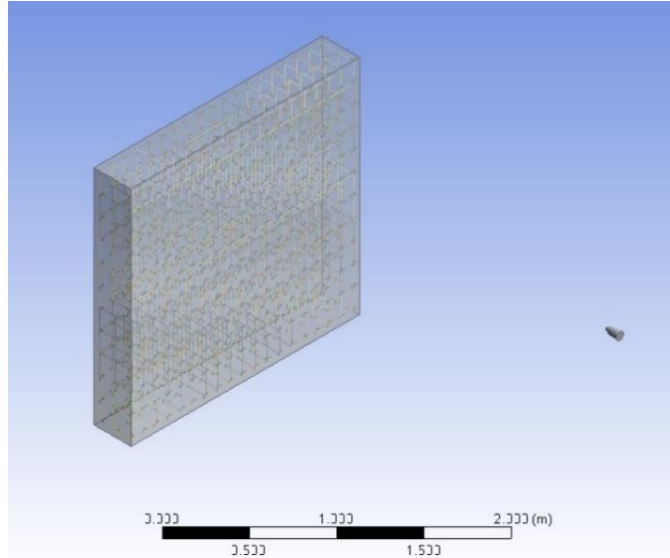
Figure 41. Reinforced Concrete Wall with Fragment due to 15.35 kg TNT Shaped Charge.
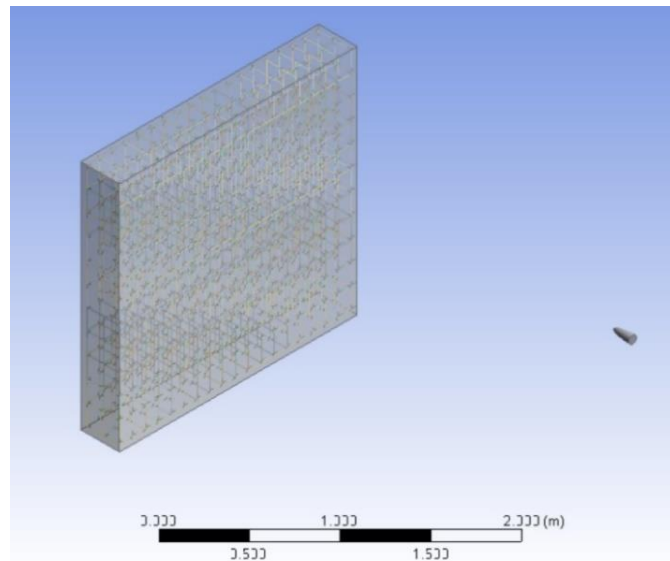
Figure 42. Reinforced Concrete Wall with Fragment due to 28.86 kg TNT Shaped Charge.

Lastly, the reinforce concrete modeled with the fragment for each case was transferred to

ANSYS AUTODYN code from ANSY Explicit Dynamic STR code shown in Figure 43 and 44.

The figures represent the final simulation settings of the impact investigation on the reinforced concrete due to TNT shaped charge in ANSYS AUTODYN code.
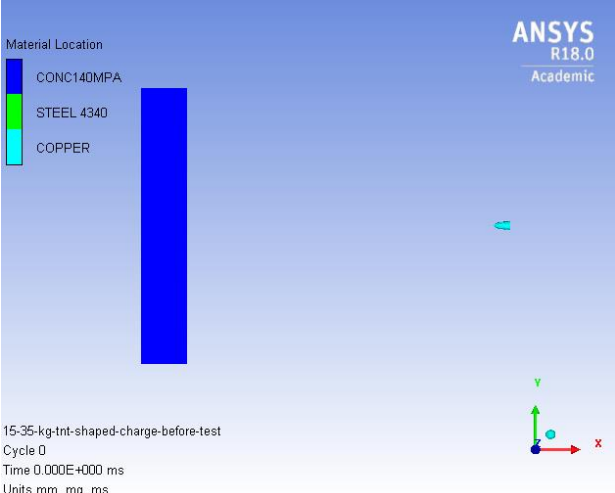
Figure 43. Final Simulation Settings of 15.35 kg TNT Shaped Charge.
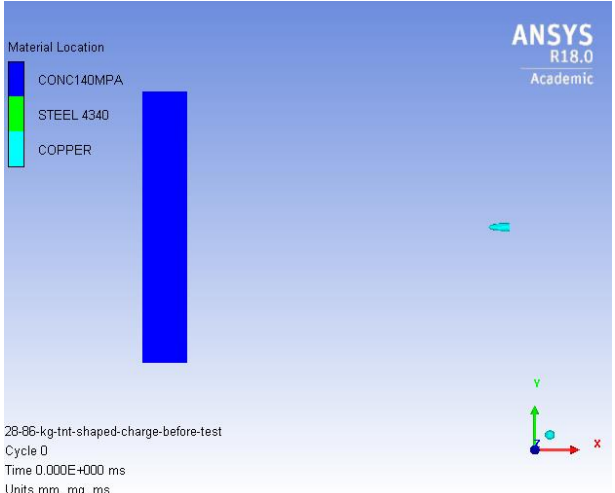
Figure 44. Final Simulation Settings of 28.86 kg TNT Shaped Charge.

After the final settings of the simulation was completed in ANSYS AUTODYN code, the fragment produce due to 15.35 kg TNT shaped charge took 24.57 ms with the incident velocity

of 2134.5 m/s in order to create an impact on the reinforced concrete model. The fragment was able to penetrate the reinforced concrete model fully, and it created a hole on the reinforced concrete model. The hole size was measured in horizontal direction using the Axes, and the hole size was 135 mm at the front side and 153 mm at the back side shown in Figure 45 and 46.
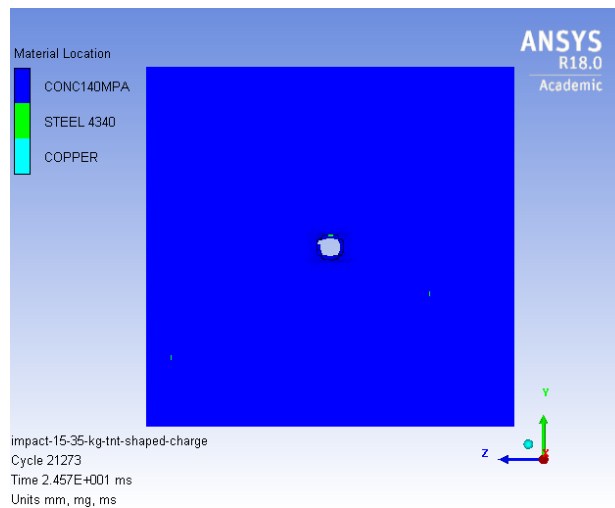
Figure 45. Hole Created at Front Side due to 15.35 kg TNT Shaped Charge.
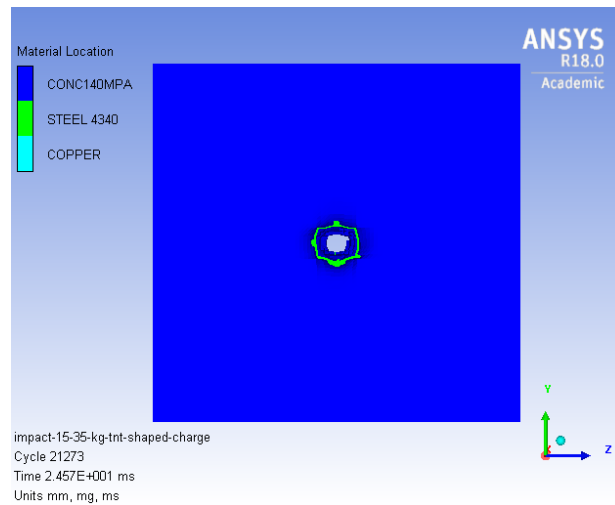
Figure 46. Hole Created at Back Side due to 15.35 kg TNT Shaped Charge.

The fragment produced due to 28.86 kg TNT shaped charge took 24.75 ms with the incident velocity of 2134.5 m/s in order to create an impact on the reinforced concrete model. The fragment was able to penetrate the reinforced concrete model fully, and it created a hole on the reinforced concrete model. The hole size was measured in horizontal direction using the Axes, and the hole size was 138 mm at the front side and 155 mm at the back side shown in Figure 47 and Figure 48.
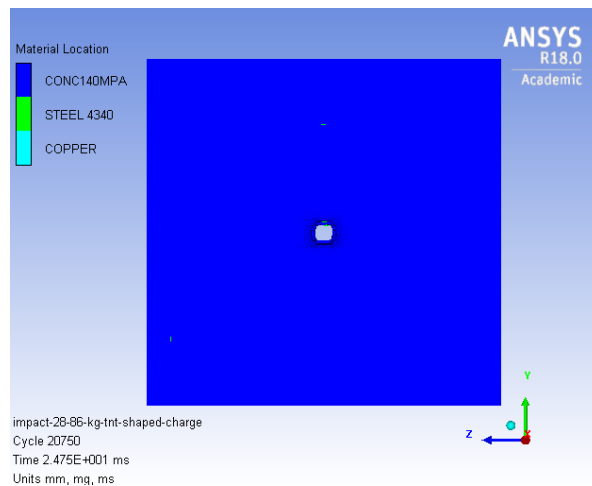
Figure 47. Hole Created at Front Side due to 28.86 kg TNT Shaped Charge.
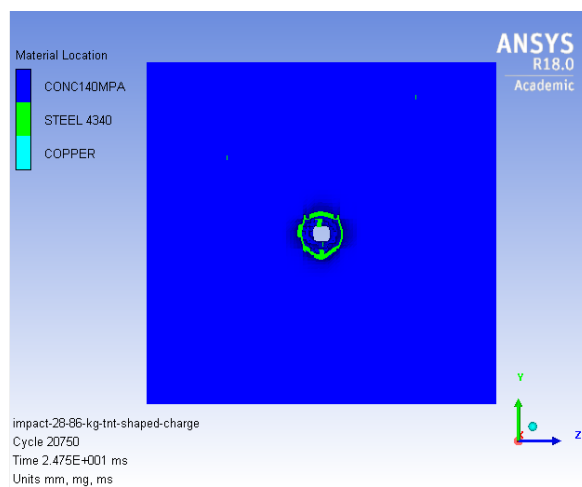
Figure 48. Hole Created at Back Side due to 28.86 kg TNT Shaped Charge.

From the parametric study of the vertical length increase for each case, the diameter and length of the fragments were increased. However, the incident velocity of the fragments were constant. Also, the size of holes were increased compared to the parametric study of the horizontal length increase. The summary of the parametric study of the vertical length increase is shown in Table 11.

Table 11. Summary Results of Vertical Length Increase.

Vertical Length Increase (mm)	Shaped Charge TNT Amount (kg)	Incident Velocity (m/s)	Estimated Size of Fragment (mm)	Front Side Hole Size (mm)	Back Side Hole Size (mm)
190	15.35	2134.5	Length: 104, Ø: 24	135	153
273	28.86	2159.6	Length: 112, Ø: 29	138	155
363	59.57	2153.2	Not Available	Not Available	Not Available

2.4.3 Parametric Study of Liner Thickness Increase

The parametric study of increasing liner thickness of TNT shaped charge was conducted. There were three cases in this parametric study. The liner thickness for each case was increased twice form the first designed TNT shaped charge. Firstly, 2D drawings were completed to calculate the amount of TNT before the numerical simulation was performed, however the calculated amount TNT was 7.64 kg for all three cases and only thickness of liners was increased, thus this step was for aiming to model visually in ANSYS AUYODYN code shown in Figures 49, 50, and Figure 51.

Figure 49. 2D Drawing of 7.64 kg TNT Shaped Charge with 9.0 mm Liner Thickness (Dimensions are in mm).

Figure 50. 2D Drawing of 7.64 kg TNT Shaped Charge with 13.5 mm Liner Thickness (Dimensions are in mm).

Figure 51. 2D Drawing of 7.64 kg TNT Shaped Charge with 18.0 mm Liner Thickness (Dimensions are in mm).

Second, the increase of the liner thickness of the TNT shaped charges were modeled and simulated using ANSYS AUTODYN code in order to obtain the incident velocity output and the size of the fragment produced due to the TNT shaped charge for each case shown in Figure 52.

TNT 7.64 kg Shaped Charge, 9mm liner thickness

TNT 7.64 kg Shaped Charge, 13.5mm liner thickness

TNT 7.64 kg Shaped Charge, 18mm liner thickness
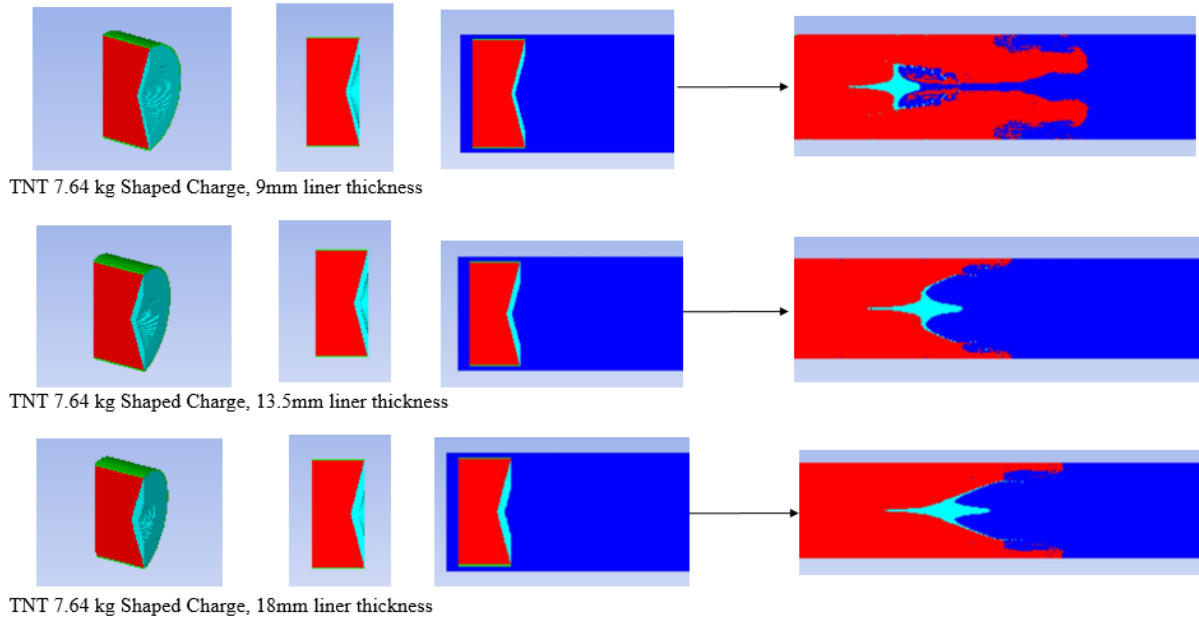
Figure 52. Parametric Studies of TNT Shaped Charges in Liner Thickness Increase.

After the simulation of the TNT shaped charges in the liner thickness increase was completed in ANSYS AUTODYN code, the incident velocity data output was obtained shown in Table 12. However, the simulation of the impact investigation was not performed in this case, because the fragment did not keep flowing forward as time passed in ANSYS AUTODYN code unlike the parametric studies of the horizontal length increase and the vertical length increase even if the fragments had a high incident velocity. One of reasons why the fragment did not flow forward for each case in this parametric study was that the amount of TNT was not enough to

make the fragment flow forward compared to its liner thickness. The thickness of liners was

increased which means the fragment mass could be increased, thus more TNT mass would be

needed to keep the fragment flowing forward (the liner thickness without increasing was 4.5

mm). Therefore, the fragment in this case assumed not to be able to reach the reinforced concrete.

The size of the fragment was not measured, but it increased as the liner thickness increased by

the sight observation compared to the parametric studies of the horizontal length increase and

vertical length increase. Thus, this parametric study was used only to observe physical

phenomena after increasing the thickness of liners.

Table 12. TNT Shaped Charges' Results as Liner Thickness Increased.

Shaped Charge TNT Amount (kg)	Liner Thickness Increase (mm)	Incident Velocity (m/s)
7.64	4.5	2039.9
7.64	9.0	1673.7
7.64	13.5	1268.8
7.64	18.0	1140.0

The incident velocity data resulted was plotted versus the TNT amount as the horizontal length increased shown in Figure 53.
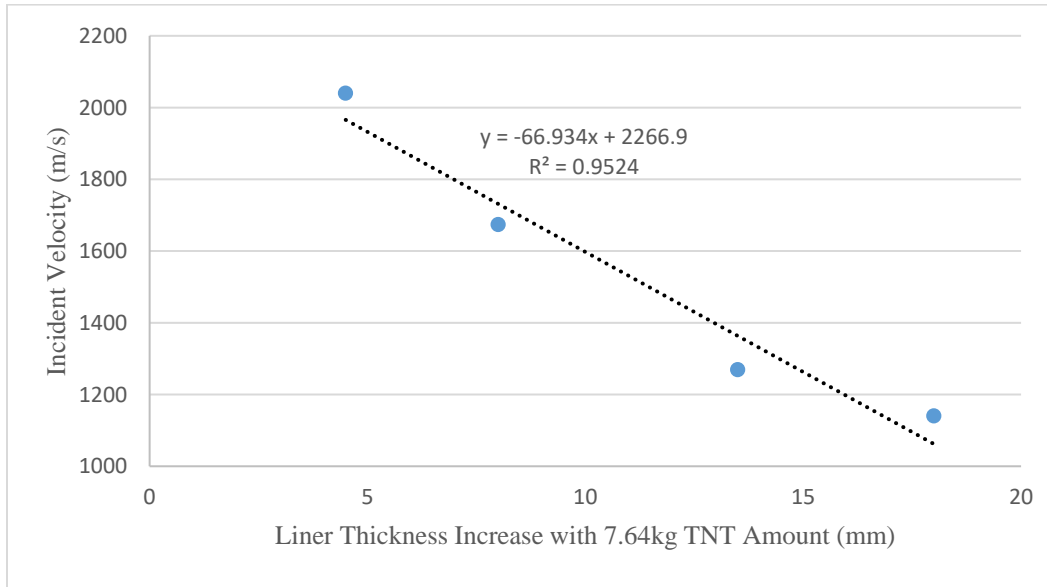
Figure 53. Incident Velocity versus TNT Amount Plot as Liner Thickness Increased with Linear Line Fitting.

Figure 53 shows the linear relationship between the incident velocity of the shaped charge and corresponding TNT mass. Considering the value of correlation coefficient, $R^2 = 0.9524$, the fitting shows a good linear relationship. Thus, the incident velocity of the shaped charge decreases as the mass of TNT with the liner thickness increases.

2.5 Final Design Considerations

From the parametric studies, the horizontal length increase resulted in the increasing of incident velocity. The vertical length increase resulted in a constant velocity, however the size of holes that was created on the reinforced concrete model was larger than the size of holes created in the parametric study of the horizontal length increase. Lastly, the liner thickness increase resulted in decreasing of the incident velocity, however the size of the fragment was the largest among these parametric studies.

Based on parametric studies and observations, the final design of the TNT shaped charge was modeled and simulated. From the parametric study of vertical length increase, the length of 273 mm was considered, and the length of 400 mm was considered from the parametric study of the horizontal length increase. This was because the length of 273 mm in the vertical length with the 28.86 kg TNT shaped charge created the largest size of the hole at the front and the back side on the reinforced concrete model, and its corresponding length in the horizontal length was 400 mm with 33.61 kg TNT shaped charge. For the liner thickness, the fragment did not flow forward in the simulation, thus the liner thickness was increased with the considered horizontal and vertical length for the final design selection.

2.5.1 Final Design Trial 1

Firstly, 2D drawings were completed to calculate the amount of TNT before the numerical simulation was performed in ANSYS AUTODYN code, and the calculated TNT amount was 143.35 kg. With this TNT amount, the liner thickness was increased as 9.0 mm and 13.5 mm shown in Figure 54 and Figure 55 respectively.
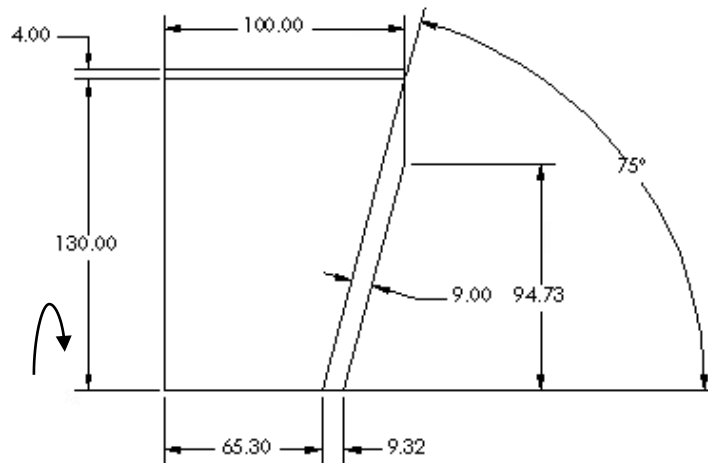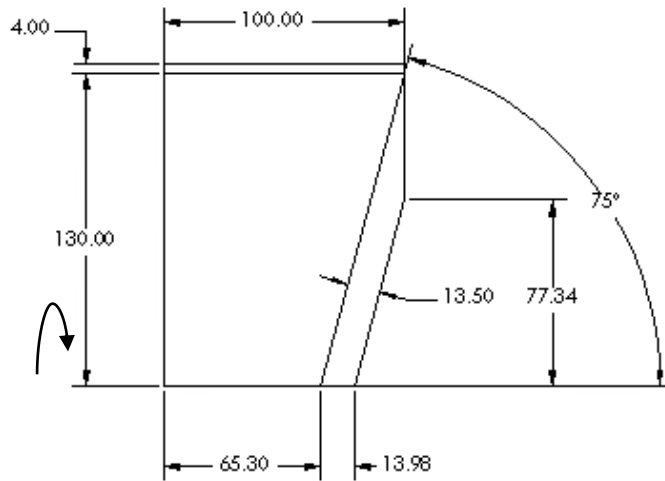
Figure 54. 2D Drawing of 143.35 kg TNT Shaped Charge with 9.0 mm Liner Thickness (Dimensions are in mm).
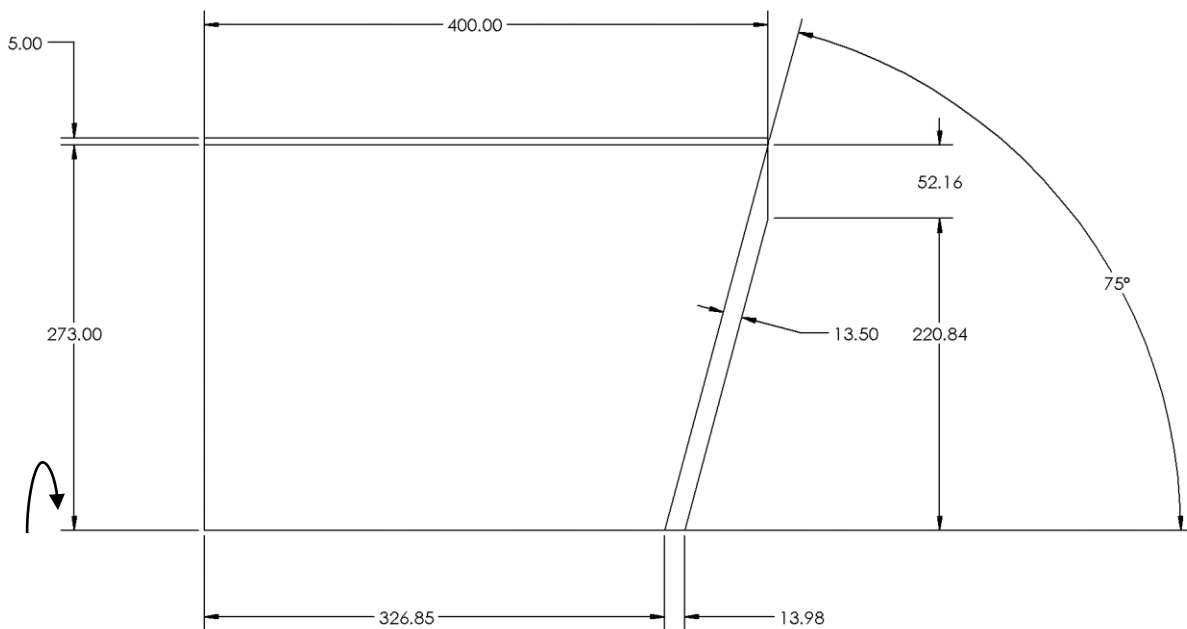
Figure 55. 2D Drawing of 143.35 kg TNT Shaped Charge with 13.5 mm Liner Thickness (Dimensions are in mm).
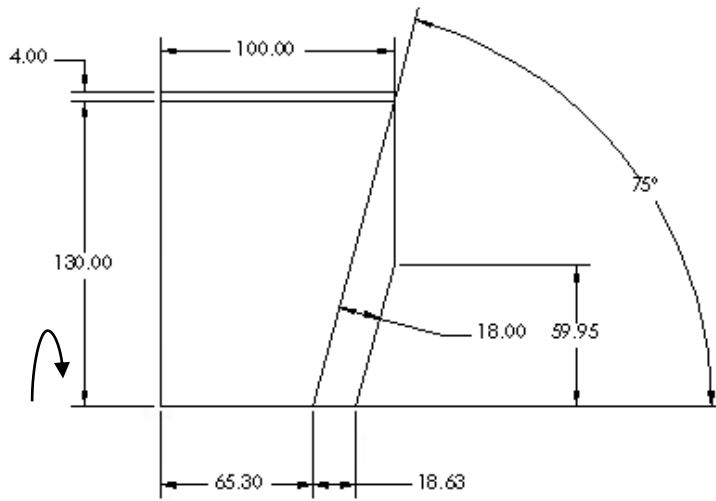
Second, the increase of the liner thickness of the TNT shaped charges with both increasing lengths in horizontal and vertical direction was modeled and simulated using ANSYS AUTODYN code in order to obtain the incident velocity output and the size of the fragment produced due to the TNT shaped charge for each case and is shown in Figure 56.

TNT 143.35 kg, 9mm liner thickness

TNT 143.45 kg, 13.5mm liner thickness

Figure 56. Final Design Trial 1 of TNT Shaped Charge with Liner Thickness Increase.

The 143.35 kg of TNT shaped charge with the 9mm liner thickness resulted in the incident velocity of 2482.3 m/s, and the size of the fragment was measured with the diameter of 37 mm and the length of 235mm. Also, the 143.35 kg of TNT shaped charge with 13.5 mm liner thickness resulted in the incident velocity of 2040.0 m/s, and the size of the fragment was measured with the diameter of 55 mm and the length of 225 mm.

After the TNT shaped charge simulation for each case was completed in ANSYS AUTODYN code, the fragment produced due to the TNT shaped charge was modeled with the reinforced concrete model in ANSYS Explicit Dynamic STR code shown in Figure 57 and Figure 58. Then, the initial conditions and boundary conditions were applied in order to perform

the impact investigation simulation due to TNT shaped charge for each case on the reinforced

concrete model in ANSYS AUTODYN code.

Figure 57. Reinforced Concrete Wall with Fragment due to 143.35 kg TNT Shaped Charge
with 9.0 mm Liner Thickness.
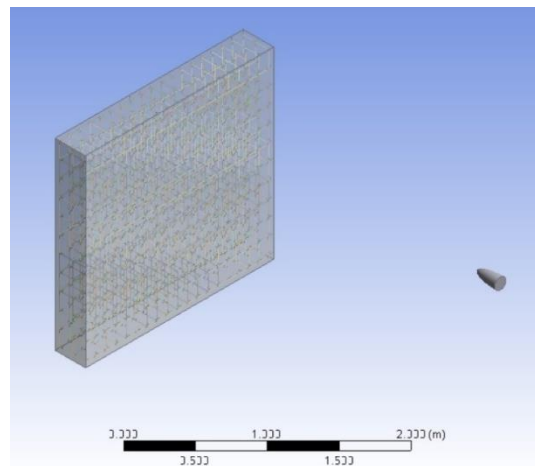
Figure 58. Reinforced Concrete Wall with Fragment due to 143.35 kg TNT Shaped Charge
with 13.5 mm Liner Thickness.

Lastly, the reinforce concrete modeled with the fragment for each case was transferred to

ANSYS AUTODYN code from ANSY Explicit Dynamic STR code shown in Figure 59 and 60.

The figures represent the final simulation settings of the impact investigation on the reinforced

concrete due to TNT shaped charge in ANSYS AUTODYN code.
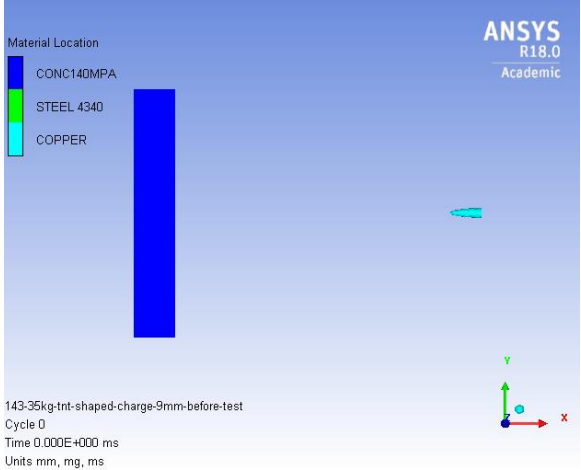
Figure 59. Final Simulation Settings of 143.35 kg TNT Shaped Charge
with 9.0 mm Liner Thickness.
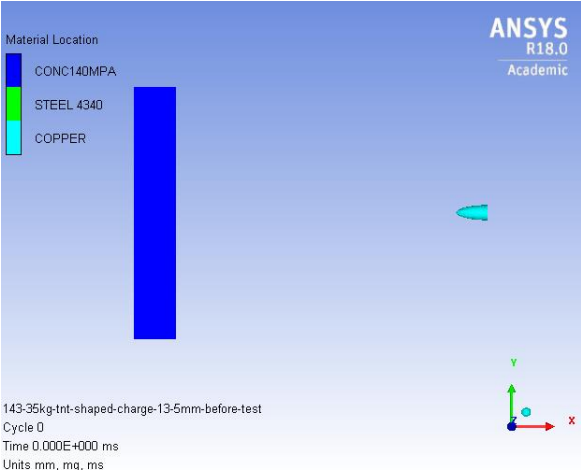
Figure 60. Final Simulation Settings of 143.35 kg TNT Shaped Charge
with 13.5 mm Liner Thickness.

After the final settings of the simulation was completed in ANSYS AUTODYN code, the

fragment produced due to 143.35 kg TNT shaped charge with 9.0 mm liner thickness took 20.99

-ms with the incident velocity of 2482.3 m/s in order to create an impact on the reinforced

concrete model. The fragment was able to penetrate the reinforced concrete model fully, and it

created a hole on the reinforced concrete model. The hole size was measured in horizontal

direction using the Axes, and the hole size was 143 mm at the front side and 162 mm at the back

side shown in Figure 61 and Figure 62.

Figure 61. Hole Created at Front Side due to 143.35 kg TNT Shaped Charge
with 9.0 mm Liner Thickness.

Figure 62. Hole Created at Back Side due to 143.35 kg TNT Shaped Charge
with 9.0 mm Liner Thickness.

143.35 kg TNT shaped charge with 13.5 mm liner thickness took 24.96 ms with the

incident velocity of 2040.0 m/s in order to create an impact on the reinforced concrete model.

The fragment was able to penetrate the reinforced concrete model fully, and it created a hole on

the reinforced concrete model. The hole size was measured in horizontal direction using the

Axes, and the hole size was 193 mm at the front side and 219 mm at the back side shown in

Figure 63 and Figure 64.

Figure 63. Hole Created at Front Side due to 143.35 kg TNT Shaped Charge
with 13.5 mm Liner Thickness.

Figure 64. Hole Created at Back Side due to 143.35 kg TNT Shaped Charge
with 13.5 mm Liner Thickness.

2.5.2 Final Design Trial 2

The resulted hole sizes of both cases were not enough that a person can pass through, thus additional simulations were performed with increasing the liner thickness. There were two cases. The first simulation was with the 143.35 kg of TNT shaped charge increasing the liner thickness of 18.0 mm, and the other simulation was with 143.35 kg of TNT shaped charge increasing the liner thickness of 22.5 mm.

Firstly, 2D drawings were completed for aiming to model visually before the numerical simulation was performed in ANSYS AUTODYN code. The 2D drawings of 143.35 kg TNT shaped charge with 18.0 mm and 143.35 kg TNT shaped charge with 22.5 mm are shown in Figure 65 and Figure 66.
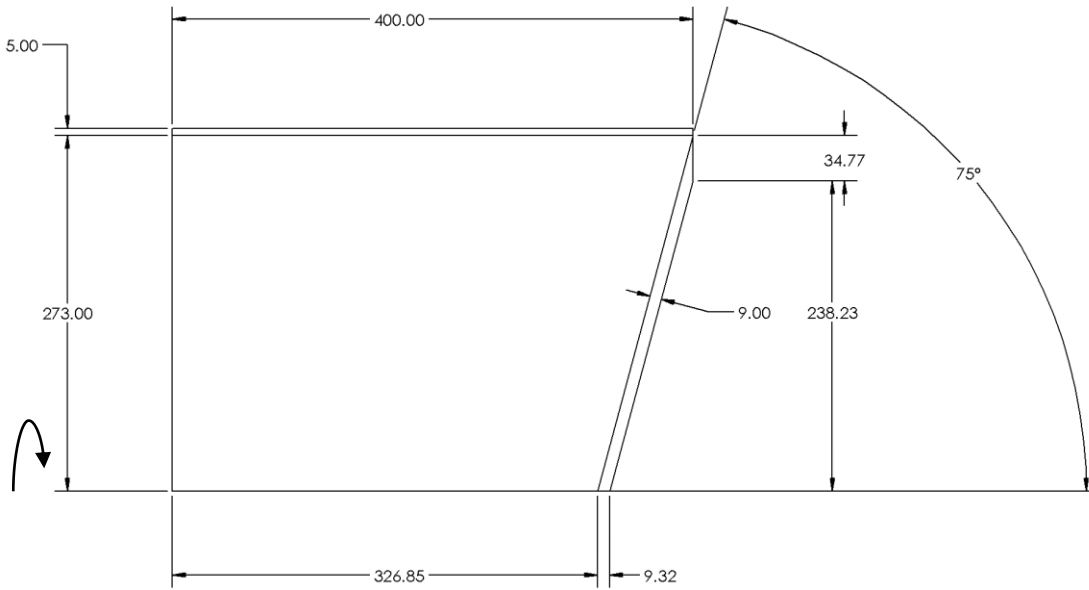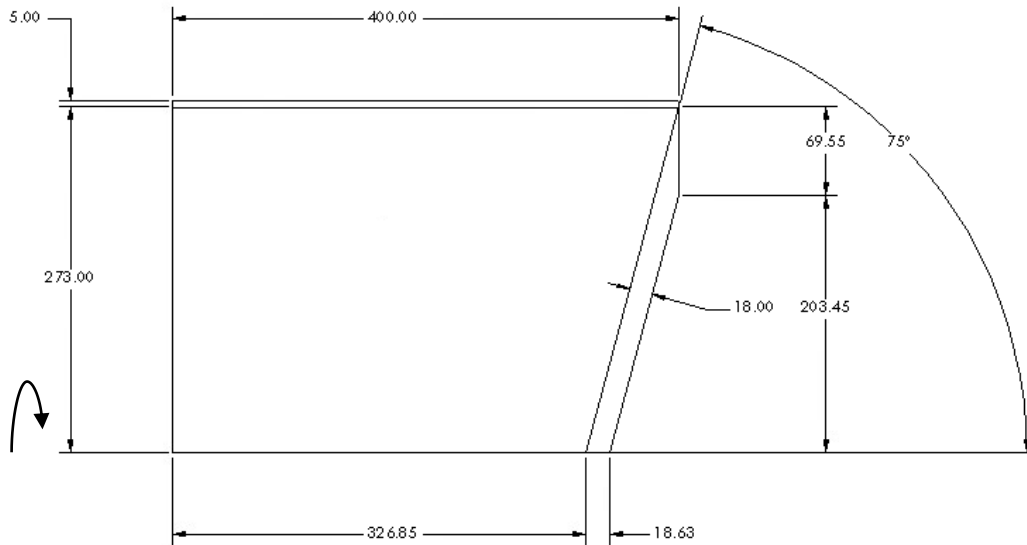

Figure 65. 2D Drawing of 143.35 kg TNT Shaped Charge with 18.0 mm Liner Thickness (Dimensions are in mm).
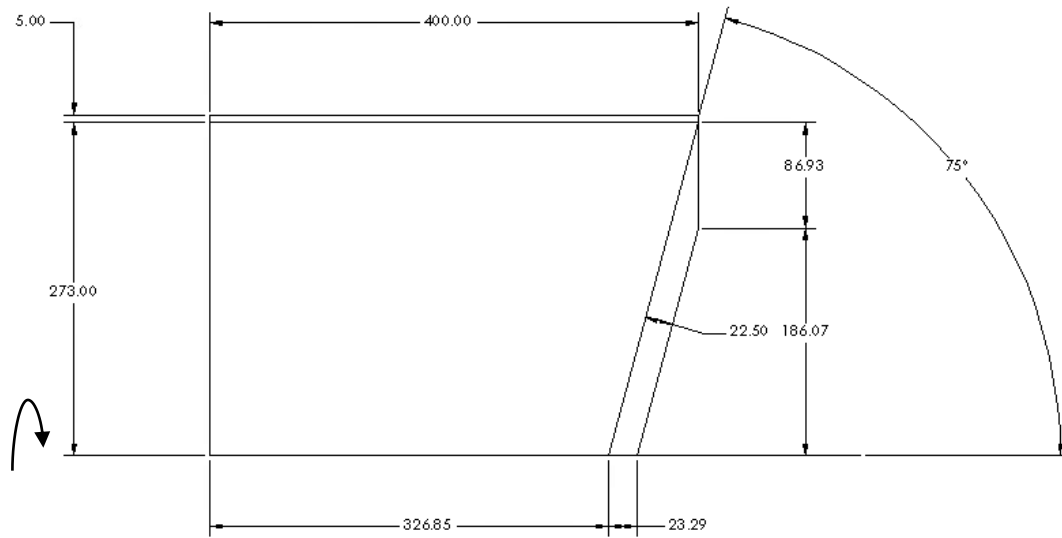
Figure 66. 2D Drawing of 143.35 kg TNT Shaped Charge with 22.5 mm Liner Thickness (Dimensions are in mm).

Second, the increase of the liner thickness of the TNT shaped charges with both increasing lengths in horizontal and vertical direction was modeled and simulated using ANSYS AUTODYN code in order to obtain the incident velocity output and the size of the fragment produced due to the TNT shaped charge for each case shown in Figure 67.

TNT 143.35 kg, 18mm liner thickness

TNT 143.35 kg, 22.5mm liner thickness
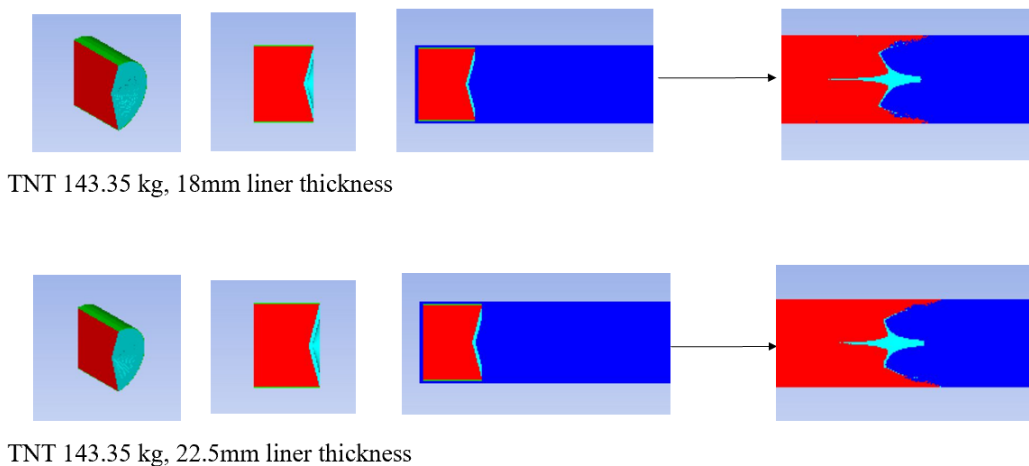
Figure 67. Final Design Trial 2 of TNT Shaped Charge with Liner Thickness Increase.

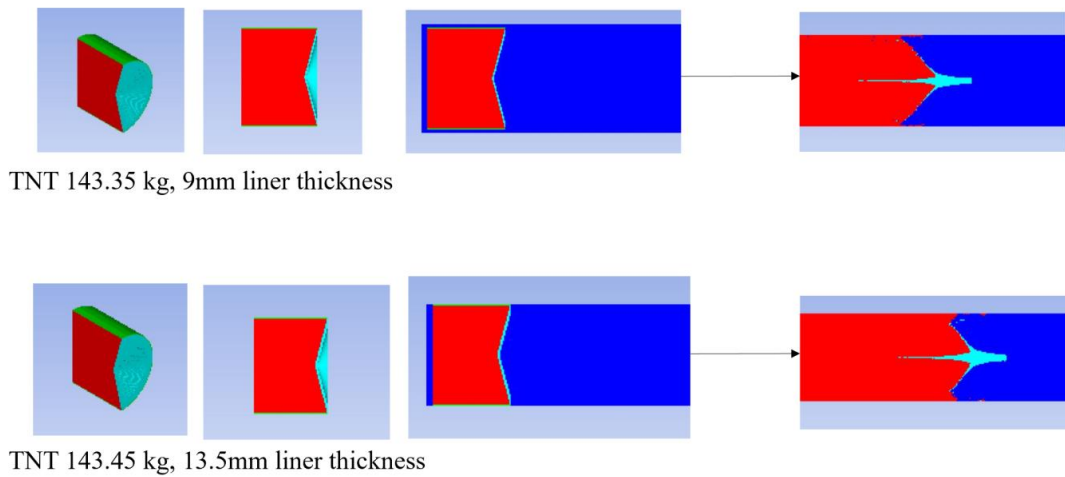The 143.35 kg of TNT shaped charge with the liner thickness of 18 mm resulted in the incident velocity of 1781.2 m/s, and the size of the fragment was measured with the diameter of 81 mm and the length of 222mm. Also, the 143.35 kg of TNT shaped charge with liner thickness of 22.5mm resulted in the incident velocity of 1060.8 m/s, and the size of the fragment was measured with the diameter of 93 mm and the length of 221 mm.

After the TNT shaped charge simulation for each case was completed in ANSYS AUTODYN code, the fragment produced due to the TNT shaped charge was modeled with the reinforced concrete model in ANSYS Explicit Dynamic STR code shown in Figure 68 and 69.
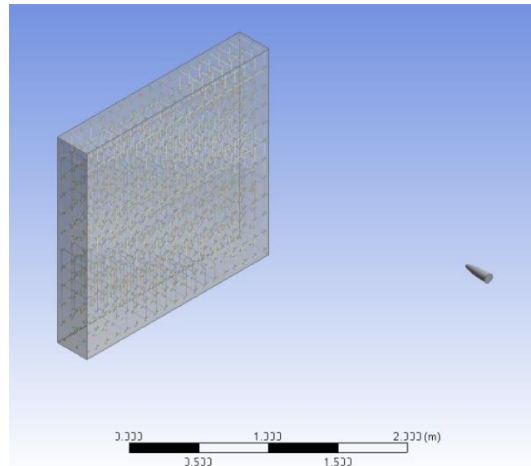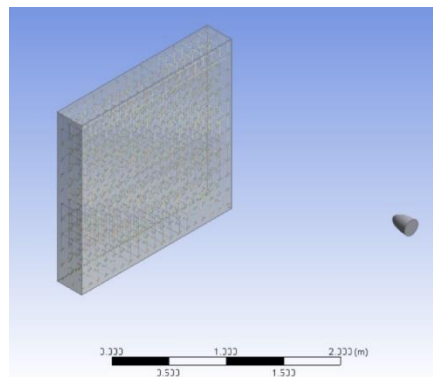

Figure 68. Reinforced Concrete Wall with Fragment due to 143.35 kg TNT Shaped Charge with 18.0 mm Liner Thickness.
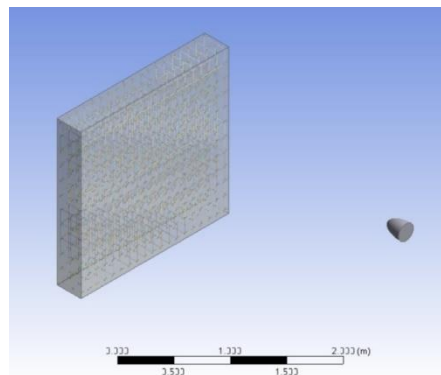
Figure 69. Reinforced Concrete Wall with Fragment due to 143.35 kg TNT Shaped Charge with 22.5 mm Liner Thickness.

Lastly, the reinforce concrete modeled with the fragment for each case was transferred to ANSYS AUTODYN code from ANSY Explicit Dynamic STR code shown in Figure 70 and 71. The figures represent the final simulation settings of the impact investigation on the reinforced concrete due to TNT shaped charge in ANSYS AUTODYN code.
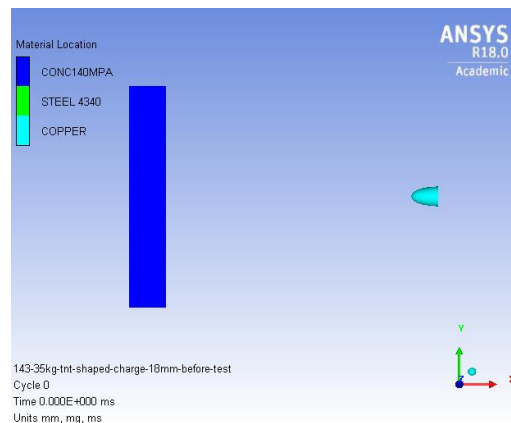
Figure 70. Final Simulation Settings of 143.35 kg TNT Shaped Charge with 18.0 mm Liner Thickness.
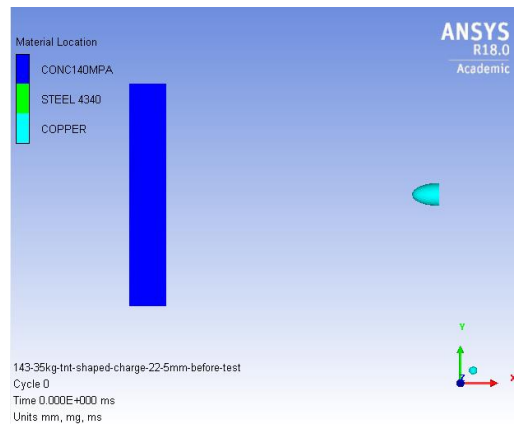
Figure 71. Final Simulation Settings of 143.35 kg TNT Shaped Charge with 22.5 mm Liner Thickness.

After the final settings of the simulation was completed in ANSYS AUTODYN code, the fragment produce due to 143.35 kg TNT shaped charge with 18.0 mm liner thickness took 28.75

-ms with the incident velocity of 1781.2 m/s in order to create an impact on the reinforced

concrete model. The fragment was able to penetrate the reinforced concrete model fully, and it

created a hole on the reinforced concrete model. The hole size was measured in horizontal

direction using the Axes, and the hole size was 252 mm at the front side and 279 mm at the back

side shown in Figure 72 and Figure 73.
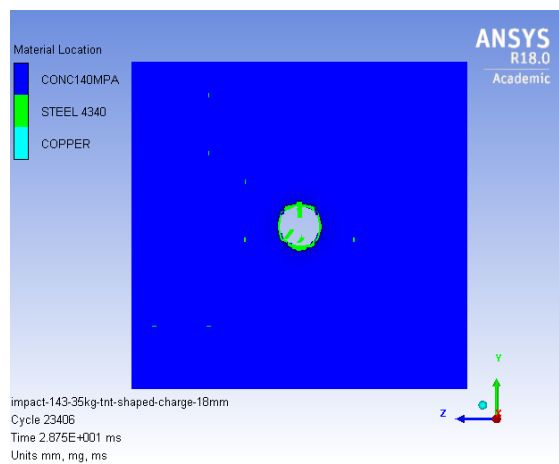
Figure 72. Hole Created at Front Side due to 143.35 kg TNT Shaped Charge
with 18.0 mm Liner Thickness.
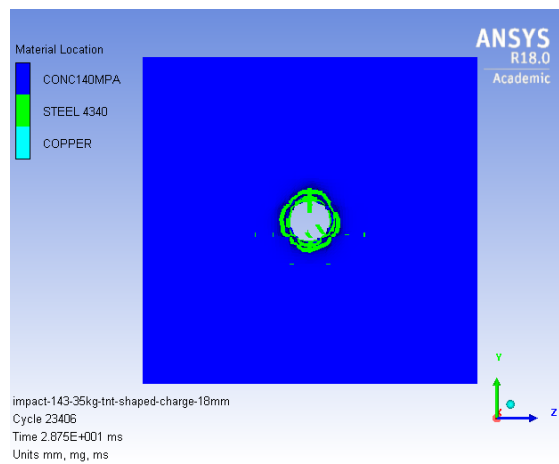
Figure 73. Hole Created at Back Side due to 143.35 kg TNT Shaped Charge
with 18.0 mm Liner Thickness.

143.35 kg TNT shaped charge with 22.5 mm liner thickness took 31.82 ms with the

incident velocity of 1060.8 m/s in order to create an impact on the reinforced concrete model.

The fragment was able to penetrate the reinforced concrete model fully, and it created a hole on

the reinforced concrete model. The hole size was measured in horizontal direction using the

Axes, and the hole size was 342 mm at the front side and 364 mm at the back side shown in

Figure 74 and Figure 75.
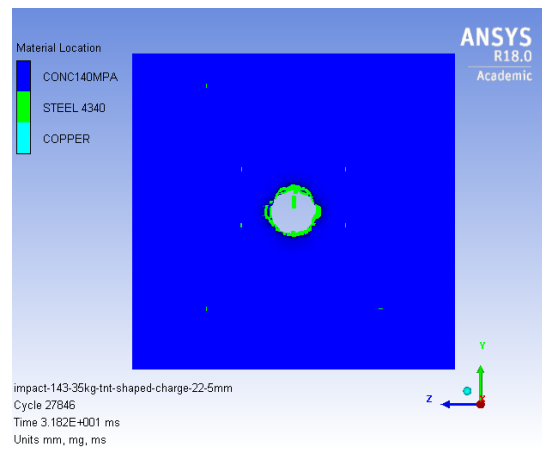
Figure 74. Hole Created at Front Side due to 143.35 kg TNT Shaped Charge
with 22.5 mm Liner Thickness.

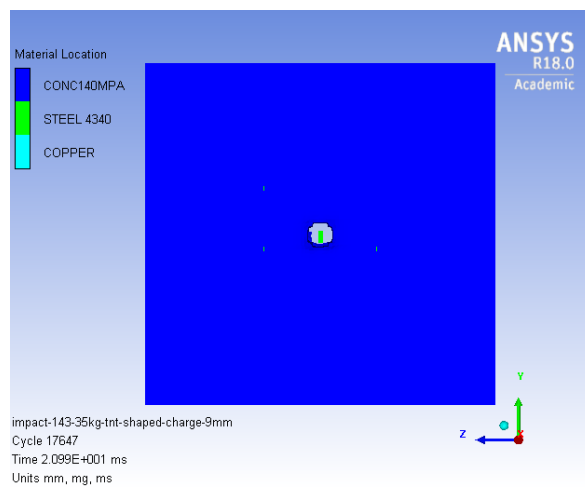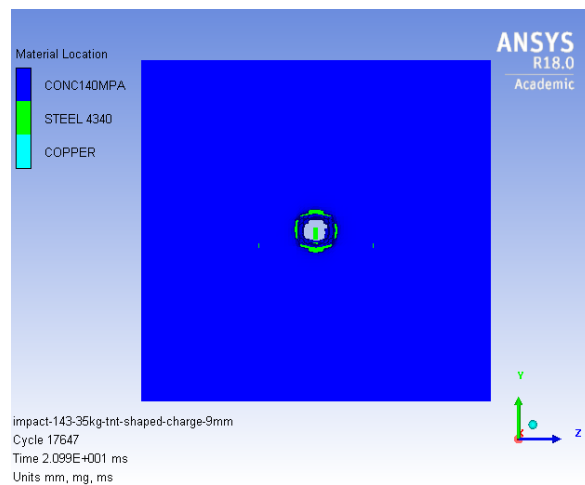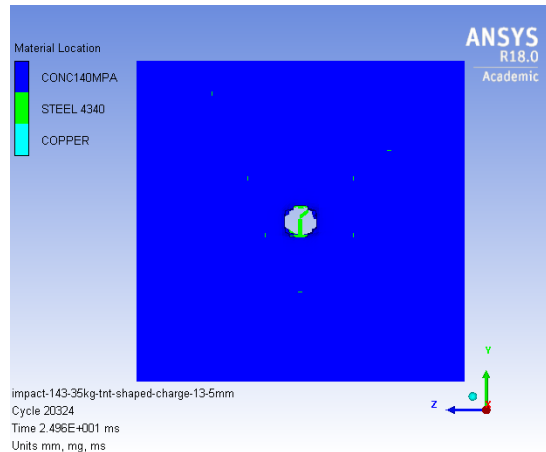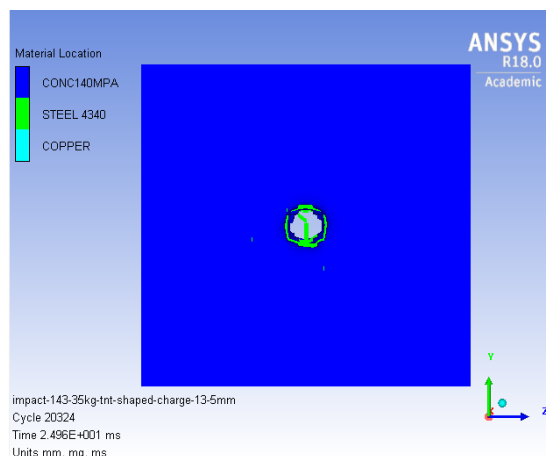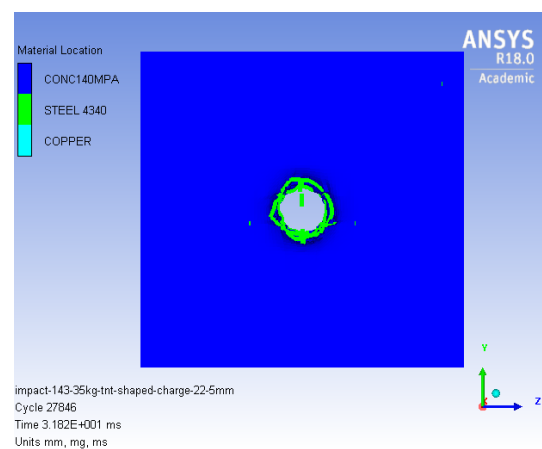Figure 75. Hole Created at Back Side due to 143.35 kg TNT Shaped Charge
with 22.5 mm Liner Thickness.

After all simulations for the final design was conducted, 143.35 kg TNT shaped Charge with 22.5 mm that the hole size created 342 mm at the front side and 364 mm at the back side on the reinforced concrete model was considered as the final design of TNT shaped charge. The summary results of final design simulations are shown in Table 13.

Table 13. Summary Results of Final Design Trials.

Shaped Charge TNT Amount (kg)	Liner Thickness Increase (mm)	Incident Velocity (m/s)	Time of Incident Velocity (ms)	Estimated Size of Fragment (mm)	Front Side Hole Size (mm)	Back Side Hole Size (mm)
143.35	9.0	2482.3	0.44249	Length: 235, Ø: 37	143	162
143.35	13.5	2040.0	0.49222	Length: 225, Ø: 55	193	219
143.35	18.0	1781.2	0.33438	Length: 222, Ø: 81	252	279
143.35	22.5	1060.8	0.33254	Length: 225, Ø: 55	342	364

This hole size was checked to perform the physical protection system (PPS) for vulnerability assessments to a hypothetical nuclear research reactor facility, and investigation of different hole size could be performed through more parametric studies. From the actual experiment of TNT shaped charge by reference paper[21], the hole size created on a steel plate target was same at the front side and the back side. However, the hole size created on the reinforced concrete model was slightly different at the front side and the back side. Possible reasons could be that steel is a homogeneous material, but the reinforced concrete is heterogeneous consisted of the concrete and reinforced steel bars. Also, concrete itself is heterogeneous material consisted of water, cement and aggregates.

3. PHYSICAL PROTECTION SYSTEM VULNERABILITY ASSESSMENTS

3.1 Vulnerability Assessments Introduction

The vulnerability of Physical Protection System (PPS) was analyzed for a hypothetical nuclear research reactor facility using Adversary Sequence Diagram (ASD) to estimate the probability of interruption (P_I) of the adversary who is attacking the facility with a shaped charge. The ASD was used to evaluate the PPS vulnerability for approaching the desired target in the research reactor facility by the adversary minimizing the probability of detection (P_D) and a delay time (t_D). Also, the calculation of P_I was for the most vulnerable path to reach the desired target.

3.2 Hypothetical Scenario Descriptions

The hypothetical scenario can be described as follows[22]:

"In this scenario, the adversary is a two-person team, and they were members of a domestic terrorist group. The group were funded $ 35,000 USD for a single attack, and their previous tactics was deceit, stealth, and diversion using car bombs and suicide bombs. Also, the group had displayed the ability to gather intelligence about target using open source collection, external surveillance of targets and through insiders. They also had displayed the ability to use covert means of communication with a very limited ability for counter surveillance. The group had proficiency with and possession of knives, handguns, semi-automatic assault rifles, and high explosives. They had access to high-grade military explosive materials. Hand and power tools, and light cars or trucks were commercially available. Lastly, the group had basic electronic skills, however they had very little radiation and radiation protection skills, limited high explosives manufacturing skills, and no viable cyber skills."

"The site consists a small research reactor on a university campus. The reactor was a 5-MW pool-type reactor using high-enriched uranium fuel. The facility consists of the reactor, associated laboratories and hot cells, and offices for employees and researchers. Outer boundary to the site is a chain link mesh fence. Outside that fence is considered offsite, and inside that fence is considered as the protected area. Employees, researchers, and visitors must wear a badge on site at all time." General sketch of the facility is shown in Figure 76.
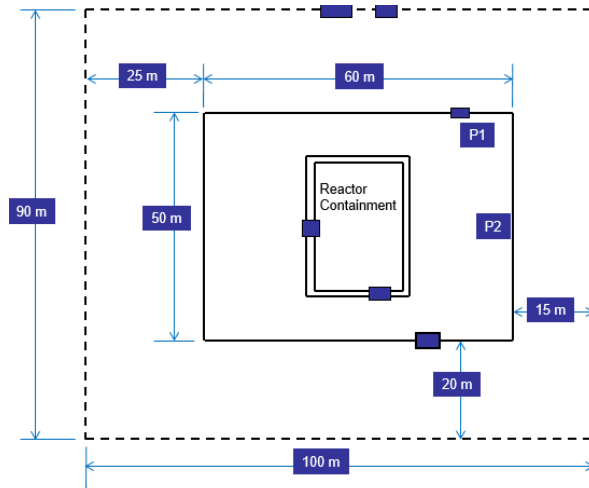
Figure 76. Dimensions of Hypothetical Nuclear Research Reactor Facility
Reprinted with Permission from[22].

"There were three guards on site at all times, and the guards worked 8 hour shifts. Normally one guard would be located at the front entrance to the building at P1 and two guards would be located in the alarm station at P2. The Response Force Time (RFT), the time that would take for the response to deploy and engage an adversary once an alarm has occurred is 90 seconds."

"For the site entrance procedure, employees, researchers and visitors would park in a parking lot at offsite, and then they would walk through the steel turnstile to enter the site. The entrance to the university campus and the access to the parking lot is open to the public.

Employees are required to use a badge swipe to unlock the turnstile. Visitors are required to

contact the guard at P2 using a telephone and identify themselves, then the guard would remotely

unlock the turnstile. Delivery vehicles are required to stop at the vehicle gate and identify

themselves to the guard at P2, then the guard would remotely unlock and open the gate for the

vehicle. All alarms for detection elements are displayed at P2, and the assessment would be

performed by camera or by deploying one of the guards from P2 to manually assess alarms."

Microwave sensors, balance magnetic switches, electromagnetic lock, and camera are used for

the exterior detection elements. General schematic of the location of guards with the exterior

elements is shown in Figure 77.
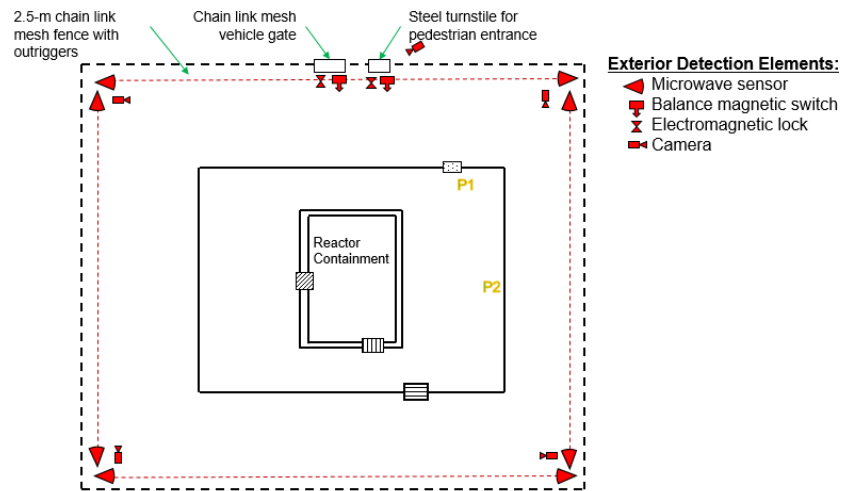
Figure 77. Location of Guards with Exterior Detection Elements
Reprinted with Permission from[22].

"The inside of the main building is consisted of offices, laboratories, storage areas, and a

loading zone. The entrance to the facility is through the entry vestibule. The reactor containment

is located in the center of the building and consisted of 30 -cm thick concrete walls with No. 4

rebar. The reactor sits in a pool within a concrete reactor pedestal that is 8-m high, and the pedestal is composed of 60 -cm concrete with No. 6 rebar. All alarms are assessed via cameras at P2 or via manual assessment by one of guards at P2." Detailed schematic of the building interior is shown in Figure 78. For detection elements in the building, microwave sensors, balance magnetic switches, and cameras are used, and detailed schematic of detection elements in the building interior is shown in Figure 79.
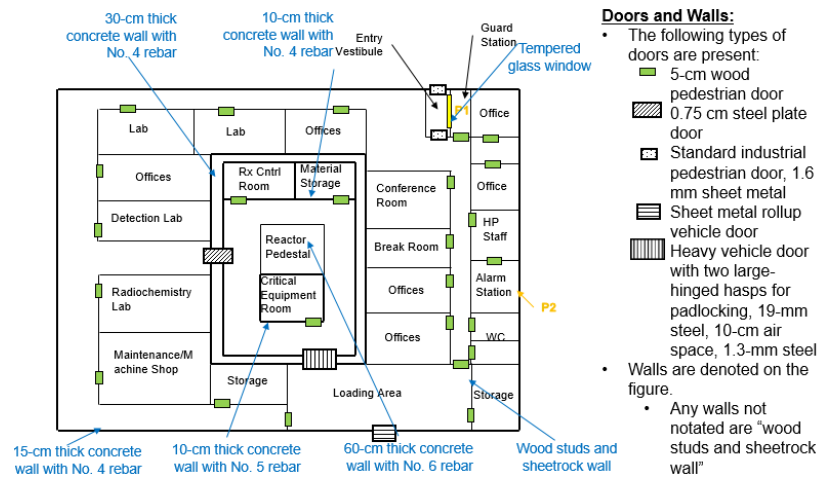
Figure 78. Detailed Schematic of Building Interior
Reprinted with Permission from[22].

Figure 79. Detailed Schematic of Detection Elements in Building Interior
Reprinted with Permission from[22].

3.3 Methodology and Procedure

The probability of interruption (P_I) of the adversary by the PPS calculation was performed in order to investigate how a nuclear facility could be weakened by outsider adversaries if they use the TNT shaped charge or other equipment to sabotage.

The first step was to create the ASD to identify the physical areas and protection layers shown in Figure 80.
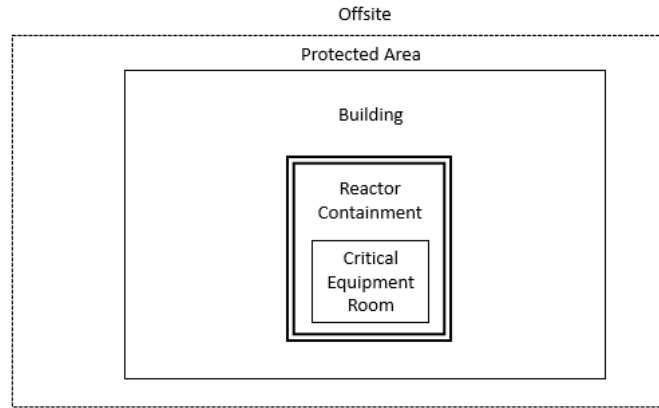
Figure 80. Schematic of Physical Areas and Protection Layers for Reactor Facility
Reprinted with Permission from[22].

Second, the ADS was constructed for the reactor. The path elements were identified for each path to enter to the critical equipment room from the offsite. Each path element had a probability of detection represented as P_D and a mean delay time represented as t_D. First, the fence-line is represented as FEN, the vehicle gate represented as VHD, and the entrance door represented as DOR from offsite to the protected area. Second, the double pedestrian door entry vestibule is represented as PER, and wall surface represented as SUR, and the metal roll up vehicle door represented as VHD from the protected are into the building. Next, there the

wooden door or steel door is represented as DOR, wall surface represented as SUR, and the

heavy vehicle door represented as VHD from the building into the reactor containment. Last,

there the wooden door is represented as DOR and wall surface represented as SUR from the

reactor containment into the critical equipment room. After traversing through a combination of

these protection elements, the adversary would be able to reach to the target shown in Figure 81.
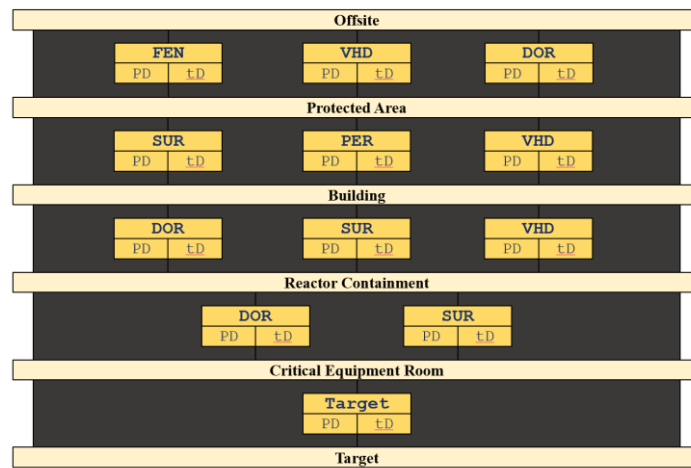
Figure 81. Adversary Sequence Diagram for Reactor
Reprinted with Permission from[22].

After the ASD for the reactor was completed, a protection element to pass through from

one physical area to the next was chosen with minimizing detection at the beginning of a task

and delay time near the end of a task. For example, choosing VHD and DOR from the offsite

into the protected area would be incorrect pathway with 100% detection, because those elements

require a badge and identification to check by a guard at P2. Therefore, the lock at the gate

remain locked without a badge and identification. Also, choosing a protection element of PER

from the protected area into the building would have essentially 100% detection for the similar

reason as that of the VHD. There is the guard at location at P1 next to PER, thus this pathway would be incorrect too. The possible selection of a protect element for each pathway is shown in Figure 82 (highlighted in yellow).
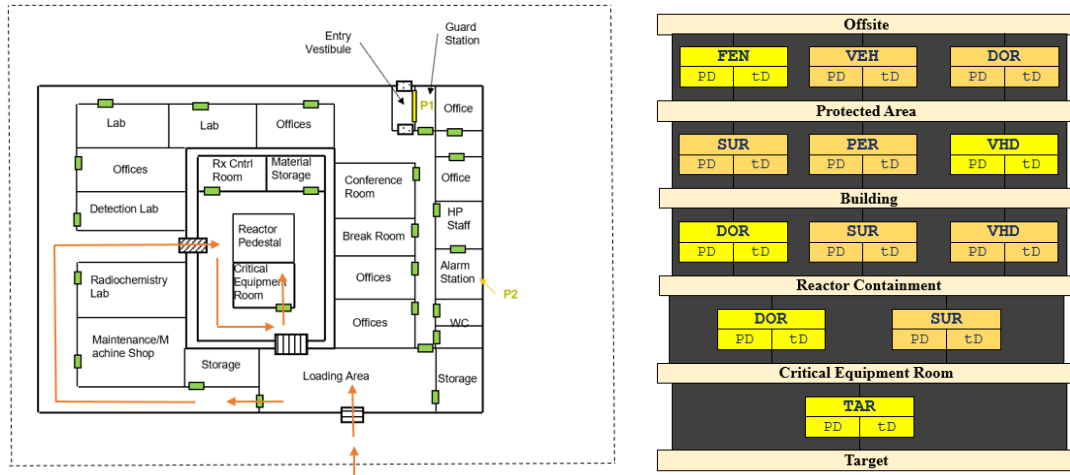
Figure 82. Adversary Sequence Diagram with Possible Adversary Sequence Paths
Reprinted with Permission from[22].

The P_I value was calculated based on the probability of detection and the probability of non-detection with assumptions of the delay time at each pathway given by[23]:

$$\beta_D^j = 1 - P_D^j \tag{8}$$

$$\beta_D = \prod_{j=1}^{J} \beta_D^j \tag{9}$$

$$P_I = 1 - \beta_D \tag{10}$$

Where, P_D^j is the probability of detection at protection element j, β_D^j is the probability of non-detection at protection element j, β_D is the combined probability of non-detection, and P_I is the probability of interruption.

In addition, the probability of interruption could be computed using Estimate of Adversary Sequence Interruption (EASI) model Excel which is a simple calculation tool that quantitatively illustrates the effect of changing physical protection parameters along a specific path.[23] A sample of EASI model input and output is shown in Table 14.

Table 14. EASI Model Sample.

	Estimate of Adversary Sequence Interruption	Probability of Interruption: 0.83			
		Probability of Alarm Communication	System Response Time (in seconds)		
			Mean	Standard Deviation	
		0.9	90	27	
Task	Description	P$_D$	Location	Delay Time (seconds)	Time Left (seconds)
				Mean	Standard Deviation	
1	Penetrates the Fence	0.7625	FEN	12	3.6	198
2	Run to the metal roll-up metal vehicle gate	0.05	VHD	10	3.0	186
3	Penetrate the vehicle gate	0.975	VHD	132	39.6	176
4	Run to the building	0.025	VHD	5	1.5	44
5	Penetrates 5-cm wooden door, run around the hallway, and penetrate 0.75-cm steel door	0.647	DOR	67	0.3	39
6	Run to the reactor containment area		DOR	5	1.5	38
7	Penetrate 5 cm wooden door to enter into the critical equipment room		DOR	12	3.6	33
8	Enter into the critical equipment room		DOR	3	0.9	21
9	Sabotage the reactor vessel Or, steal special nuclear materials		Target	18	5.4	18

In this paper, the probability of interruption was calculated only for the vulnerability assessments to the hypothetical nuclear research reactor facility if adversary used TNT shaped charge for approaching the desired target. However, the vulnerability assessments can be analyzed further by the estimation of risk which calculates the survival rate of the adversary. The estimation of the risk to the facility of an adversary gaining access to, or stealing, critical assets is given by[23]:

$$\text{Risk} = P_{Attack} * [1 - (P_{Interruption} P_{Neutralization})] * C \tag{9}$$

Where, P_{Attack} is the probability of an adversary attack during a period of time with the value from 0 (no chance at all of attack) to 1.0 (certainty of attack), $P_{Interruption}$ is the probability of interruption with the value from 0 (no chance at all of interruption) to 1.0 (certainty of interruption), $P_{Neutralization}$ is the probability of neutralizing the adversary by the guards with the value from 0 (no chance at all of neutralizing the adversary) and 1.0 (certainty of neutralizing the adversary), and C is the consequence of the loss by the attack with the value from 0 (no chance at all of consequence) to 1.0 (certainty consequence).

In the estimation of risk, the value of P_{Attack} and C is subjective, and only the value of $P_{Interruption}$ and $P_{Neutralization}$ can be calculated for the estimation. The probability of interruption, could be improved by the probability of detection and delay time depending on where the adversary chooses the paths. The probability of neutralization, $P_{Neutralization}$, could be depended on physical protection systems in the facility such as detection elements and the force response time by guards as an example. Thus, these two terms are effective for the survival rate of the adversary, and this analysis can be worked as a future work.

3.4 Assumptions for Calculation of Probability of Interruption

There were several assumptions to calculate the probability of interruption for the given P_D and t_D values of each protection element along the adversary path. These assumptions were made based on the sample pathway shown in Figure 82.[22,23]

1. Response Force Time (RFT) was assumed to be 90 seconds.

2. The standard deviation for all assumed delay times to be 30%.

3. From the offsite to the protected area:

   - From the delay times tables, a mean time of 12 s was assumed to penetrate the fence (FEN), followed by 10 s to crawl past the microwave sensor and run the rest of the 20 -m to the vehicle door of the building. Also, a chance of being seen by the cameras was assumed to be 5% during this 10 s.

   - FEN: 2.5 -m chain link mesh fence with outriggers.

   - Camera and Microwave Sensor down each fence-line.

   - P_D for crawling through microwave sensor is (M-H) 0.5-0.7 for one person. For 2 intruders the microwave sensors non-detection probability,

     $\beta_D = (0.5)(0.5) = 0.25 \rightarrow P_D = 0.75$.

   - Additionally, there might be a 5% chance of being seen by the cameras while climbing the fence. $\beta_D = (0.25)(0.95) = 0.2375 \rightarrow P_D = 0.7625$.

4. From the protected area to the building:

   - Entry vestibule consisted of two personnel doors, microwave sensor, balance magnetic switch, camera, and guard. $P_D \approx 0.95$.

   - Wall surface was 15 -cm thick concrete with No.4 rebar. $P_D \approx 0.95$. This task would not be possible to penetrate without explosives.

- VHD: Sheet metal rollup vehicle door, mean delay time was assumed to of 132 s to penetrate sheet metal rollup vehicle door with fire ax, no detection by balanced magnetic switch. Approximately 65% chance of being detected by the passive camera was assumed during this 132 s. $P_D = 0.65$

- Then about 5 s to run to the building. A chance of being seen by the cameras was assumed to be 0.025% during this 5 s. $P_D = 0.025$

5. From the building to the reactor containment:

- SUR: 30 -cm thick concrete wall with No. 4 rebar. $P_D \approx 0.95$.

  This task would not be possible to penetrate without explosives.

- VHD: Heavy vehicle door 19 -mm steel, 10 -cm air space, 1.3-mm steel. Two large-hinged hasps and high-security padlocks from the inside. To penetrate the heavy vehicle door would require an equipment the weight of which is not possible for the adversary to carry

- DOR: This path would include penetrating the 5 -cm wood pedestrian door to the building hallway, running around the hallway to the 0.75 -cm steel plate door, and penetrating the 0.75 -cm steel plate door to enter the reactor containment.

  1. The adversary would penetrate the 5 -cm wood pedestrian door to the hallway assuming the mean delay time of 12 s to penetrate the 5 -cm wood door with fire ax, and also there is a chance of being seen by the passive camera and was assumed to be 5% during this task. $P_D = 0.05$.

  2. The adversary would run around the hallway to the 0.75 -cm steel plate door with assuming 25 s to run the hallways to the door, passive camera. $P_D = 0.125$.

79

3. The adversary would penetrate the 0.75 -cm steel plate door to enter the reactor containment assuming the mean delay time of 30 s to penetrate with cutting torch, passive camera. $P_D = 0.15$.

Total delay time would be 67 s to enter reactor containment with all these tasks, also assuming a $P_D = 0.5$ from drawing attention within the building.

Therefore, $\beta_D = (0.95)(0.875)(0.85)(0.5) = 0.353 \rightarrow P_D = 0.647$.

6. From the reactor containment into the critical equipment room

- SUR: 10 -cm thick concrete wall with No.5 rebar. $P_D \approx 0.95$.

  This task would not be possible without explosives.

- DOR: 5 -cm wood pedestrian door with balance magnetic switch and electromagnetic lock assuming the mean delay time of 12 s to penetrate door with fire ax, and additional 3 s to run to the target before the 18 s to set the 10 kg explosive.

3.5 Calculation of Probability of Interruption for Several Pathways

Unlike the sample pathway, the adversary would be able to use TNT shaped charges in order to sabotage the nuclear facility or steal SNM after they were able to break into the facility. A venerability analysis for calculating the P_I was performed with the detailed information of the hypothetical facility plan. There were three different pathways for this analysis in order to investigate the most vulnerable paths for this facility.

3.5.1 Calculation of Probability of Interruption for Pathway 1

The ASD was created with the adversary sequence paths to minimize the delay time and the probability of detection shown in Figure 83, and required tasks for the adversary are shown below.

Figure 83. Adversary Sequence Diagram for Pathway 1
Reprinted with Permission from[22].

1. Task 1, from the offsite to the protected area:

   - From the delay times tables, a mean time of 12 s was assumed to penetrate the fence, followed by 10 s to crawl past the microwave sensor and run the rest of the 20 -m to the vehicle door of the building. Also, a chance of being seen by the cameras was assumed to be 5% during this 10 s.

   - FEN: 2.5 -m chain link mesh fence with outriggers.

   - Camera and Microwave Sensor down each fence-line.

   - P_D for crawling through microwave sensor is (M-H) 0.5-0.7 for one person. For 2 intruders the microwave sensors non-detection probability,

     $\beta_D = (0.5)(0.5) = 0.25 \rightarrow P_D = 0.75$.

   - Additionally, there might be a 5% chance of being seen by the cameras while climbing the fence. $\beta_D = (0.25)(0.95) = 0.2375 \rightarrow P_D = 0.7625$.

2. Task 2, from the protected area to the building:

   - VHD: Sheet metal rollup vehicle door, mean delay time was assumed to of 132 s to penetrate sheet metal rollup vehicle door with fire ax, no detection by balanced magnetic switch. Approximately 65% chance of being detected by the passive camera was assumed during this 132 s. $P_D = 0.65$

   - Then about 5 s to run to the building. A chance of being seen by the cameras was assumed to be 0.025% during this 5 s. $P_D = 0.025$

3. Task 3, from the building to the reactor containment:

   - SUR: 30 -cm thick concrete wall with No. 4 rebar. $P_D \approx 0.95$.

     The adversary would use a TNT shaped charge to penetrate the concrete wall assuming 1 s to penetrate, also a $P_D = 0.5$ from drawing attention within the building.

Therefore, $\beta_D = (0.05)(0.5) = 0.025 \rightarrow P_D = 0.975$

4. Task 4, from the reactor containment into the critical equipment room

- DOR: 5 -cm wood pedestrian door with balance magnetic switch and electromagnetic

  lock assuming the mean delay time of 12 s to penetrate door with fire ax, and

  additional 3 s to run to the target before the 18 s to set the 10 kg explosive.

The value of P_I for this pathway was calculated with these assumptions, P_D, t_D, RFT using EASI model Excel tool shown in Table 14, and the calculated value of P_I value was 0.70.

Table 15. Calculation of Probability of Interruption for Pathway 1 Using EASI Model.

Estimate of Adversary Sequence Interruption		Probability of Interruption: 0.70				
		Probability of Alarm Communication	System Response Time (in seconds)			
			Mean	Standard Deviation		
		0.9	90	27		
Task	Description	P_D	Location	Delay Time (seconds)		Time Left (seconds)
				Mean	Standard Deviation	
1	Penetrates the Fence	0.7625	FEN	12	3.6	198
2	Run to the metal roll-up vehicle gate	0.05	VHD	10	3.0	186
3	Penetrate the vehicle gate	0.65	VHD	132	39.6	176
4	Run to the building	0.025	VHD	5	1.5	44
5	Penetrates 30 -cm thick concrete wall using TNT shaped charge to enter into the reactor containment area	0.975	SUR	1	0.3	39
6	Run to the reactor containment area		SUR	5	1.5	38
7	Penetrate 5 -cm wooden door to enter into the critical equipment room		DOR	12	3.6	33
8	Enter into the critical equipment room		DOR	3	0.9	21
9	Sabotage the reactor vessel		Target	18	5.4	18

3.5.2 Calculation of Probability of Interruption for Pathway 2

The adversary sequence diagram was created with the adversary sequence paths to minimize the delay time and the probability of detection shown in Figure 84, and required tasks for the adversary are shown below.
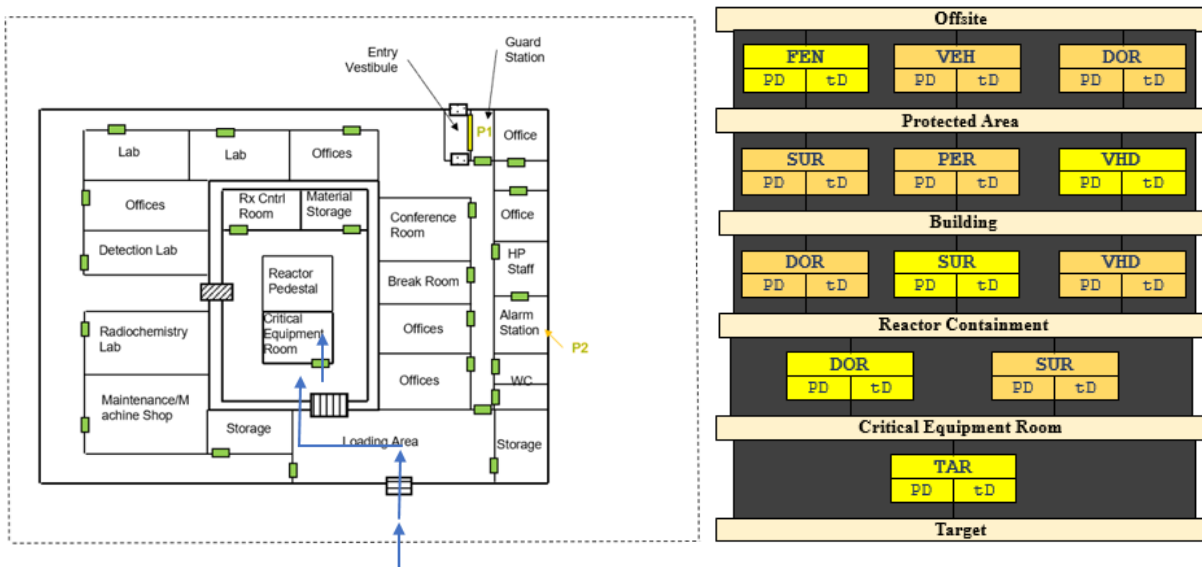

Figure 84. Adversary Sequence Diagram for Pathway 2
Reprinted with Permission from[22].

1. Task 1, from the offsite to the protected area:

   • From the delay times tables, a mean time of 12 s was assumed to penetrate the fence, followed by 10 s to crawl past the microwave sensor and run the rest of the 20 -m to the vehicle door of the building. Also, a chance of being seen by the cameras was assumed to be 5% during this 10 s.

   • FEN: 2.5-m chain link mesh fence with outriggers.

   • Camera and Microwave Sensor down each fence-line.

84

- P_D for crawling through microwave sensor is (M-H) 0.5-0.7 for one person. For 2 intruders the non-detection probability of the microwave sensors,

  $\beta_D = (0.5)(0.5) = 0.25 \rightarrow P_D = 0.75$.

- Additionally, there might be a 5% chance of being seen by the cameras while climbing the fence. $\beta_D = (0.25)(0.95) = 0.2375 \rightarrow P_D = 0.7625$.

2. Task 2, from the protected area to the building:

- Wall surface was 15 -cm thick concrete with No.4 rebar. $P_D \approx 0.95$.

  The adversary would use a TNT shaped charge to penetrate the concrete wall assuming 1 s to penetrate, also a $P_D = 0.5$ from drawing attention within the building. Therefore, $\beta_D = (0.05)(0.5) = 0.025 \rightarrow P_D = 0.975$

- Then about 5 s to run to the building. A chance of being seen by the cameras was assumed to be 0.025% during this 5 s. $P_D = 0.025$

3. Task 3, from the building to the reactor containment:

- DOR: This path would include penetrating the 5 -cm wood pedestrian door to the building hallway, running around the hallway to the 0.75-cm steel plate door, and penetrating the 0.75 -cm steel plate door to enter the reactor containment.

  1. The adversary would penetrate the 5 -cm wood pedestrian door to the hallway assuming the mean delay time of 12 s to penetrate the 5 -cm wood door with fire ax, and also a chance of being seen by the passive camera was assumed to be 5% during this task. $P_D = 0.05$.

  2. The adversary would run around the hallway to the 0.75 -cm steel plate door with assuming 25 s to run the hallways to the door, passive camera. $P_D = 0.125$.

3. The adversary would penetrate the 0.75 -cm steel plate door to enter the reactor containment assuming the mean delay time of 30 s to penetrate with cutting torch, passive camera. $P_D = 0.15$.

Total delay time would be 67 s to enter reactor containment with all these tasks, also assuming a $P_D = 0.5$ from drawing attention within the building.

Therefore, $\beta_D = (0.95)(0.875)(0.85)(0.5) = 0.353 \rightarrow P_D = 0.647$.

4. Task 4, from the reactor containment into the critical equipment room

- DOR: 5 -cm wood pedestrian door with balance magnetic switch and electromagnetic lock assuming the mean delay time of 12 s to penetrate door with fire ax, and additional 3 s to run to the target before the 18 s to set the 10 kg explosive.

The value of P_I for this pathway was calculated with these assumptions, P_D, t_D, RFT using EASI model Excel tool shown in Table 15, and the calculated value of P_I value was 0.76.

Table 16. Calculation of Probability of Interruption for Pathway 2 Using EASI Model.

Estimate of Adversary Sequence Interruption		Probability of Interruption: 0.76				
		Probability of Alarm Communication	System Response Time (in seconds)			
			Mean	Standard Deviation		
		0.9	90	27		
Task	Description	P_D	Location	Delay Time (seconds)		Time Left (seconds)
				Mean	Standard Deviation	
1	Penetrates the Fence	0.7625	FEN	12	3.6	133
2	Run to the metal roll-up vehicle gate	0.05	VHD	10	3.0	121
3	Penetrate 15 -cm thick concrete wall next to the vehicle gate using TNT shaped charge to enter into the building	0.975	SUR	1	0.3	111
4	Run to the building	0.025	SUR	5	1.5	110
5	Penetrate 5 -cm wooden door, run around the hallway, penetrate 0.75 -cm steel door to enter into the reactor containment area	0.647	DOR	67	20.1	105
6	Run to the reactor containment area		DOR	5	1.5	38
7	Penetrate the 5 -cm wooden door to enter into the critical equipment room		DOR	12	3.6	33
8	Enter into the critical equipment room		DOR	3	0.9	21
9	Sabotage the reactor vessel		Target	18	5.4	18

3.5.3 Calculation of Probability of Interruption for Pathway 3

  The adversary sequence diagram was created with the adversary sequence paths to minimize the delay time and the probability of detection shown in Figure 85, and required tasks for the adversary are shown below.
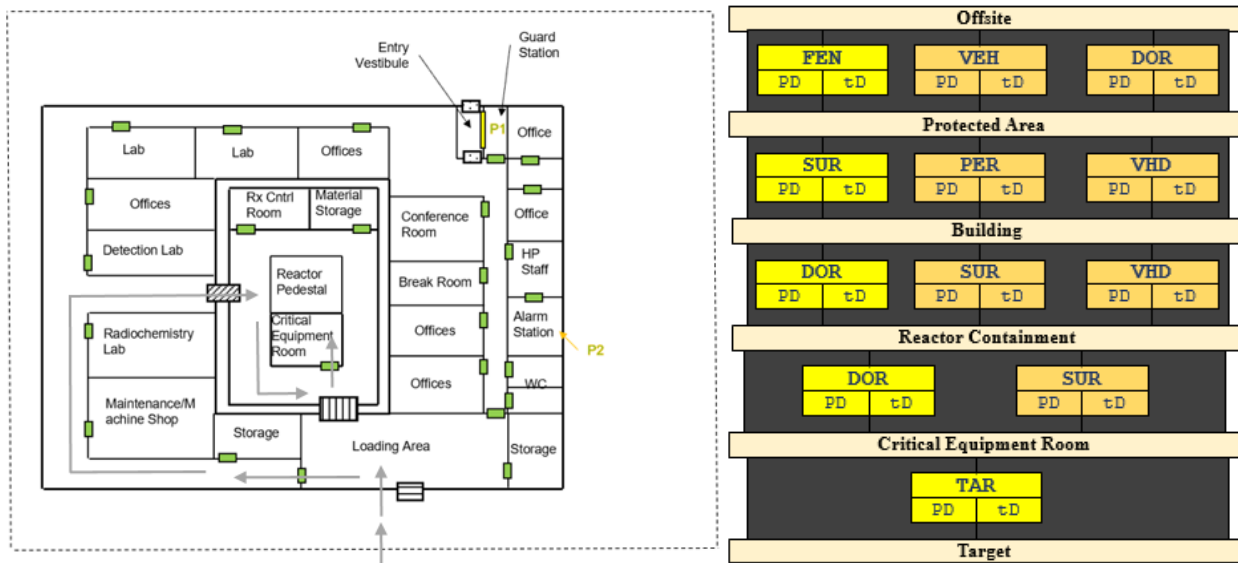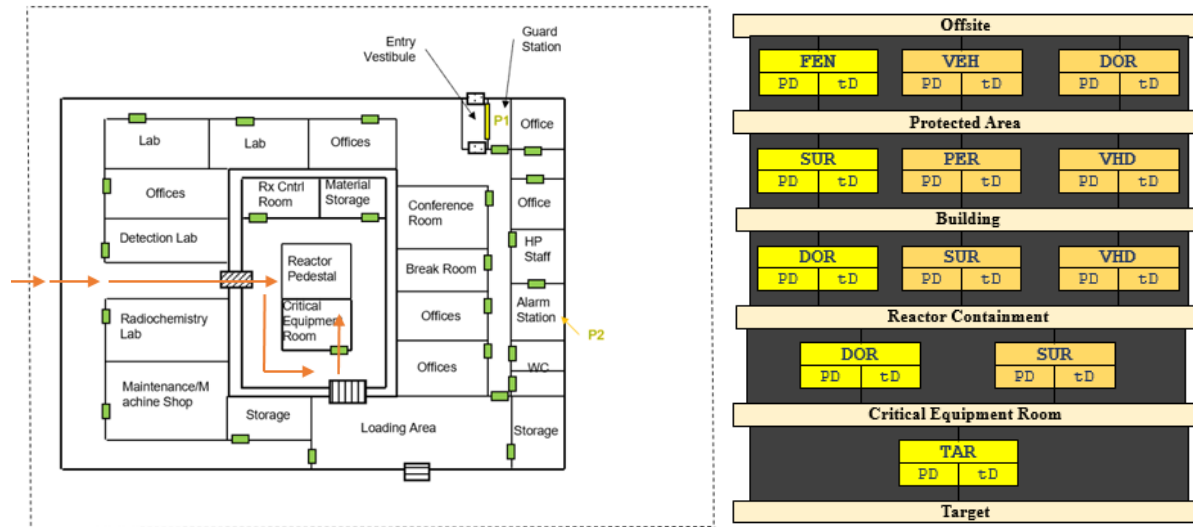

Figure 85. Adversary Sequence Diagram for Pathway 3
Reprinted with Permission from[22].

1. Task 1, from the offsite to the protected area:

   - From the delay times tables, a mean time of 12 s was assumed to penetrate the fence, followed by 10 s to crawl past the microwave sensor and run the rest of the 20-m to the vehicle door of the building. Also, a chance of being seen by the cameras was assumed to be 5% during this 10 s.

   - FEN: 2.5 -m chain link mesh fence with outriggers.

   - Camera and Microwave Sensor down each fence-line.

- P_D for crawling through microwave sensor is (M-H) 0.5-0.7 for one person. For 2 intruders the non-detection probability of the microwave sensors,

  $\beta_D = (0.5)(0.5) = 0.25 \rightarrow P_D = 0.75$.

- Additionally, there might be a 5% chance of being seen by the cameras while climbing the fence. $\beta_D = (0.25)(0.95) = 0.2375 \rightarrow P_D = 0.7625$.

2. Task 2, from the protected area to the building:

- Wall surface was 15 -cm thick concrete with No.4 rebar. $P_D \approx 0.95$.

  The adversary would use a TNT shaped charge to penetrate the concrete wall assuming 1 s to penetrate, also a $P_D = 0.5$ from drawing attention within the building. Therefore, $\beta_D = (0.05)(0.5) = 0.025 \rightarrow P_D = 0.975$

- Then about 5 s to run to the building. A chance of being seen by the cameras was assumed to be 0.025% during this 5 s. $P_D = 0.025$

3. Task 3, from the building to the reactor containment:

- DOR: This path would include running around the hallway to the 0.75 -cm steel plate door, and penetrating the 0.75 -cm steel plate door to enter the reactor containment.

  1. The adversary would run around the hallway to the 0.75 -cm steel plate door with assuming 5 s to run the hallways to the door, passive camera. $P_D = 0.125$.

  2. The adversary would penetrate the 0.75 -cm steel plate door to enter the reactor containment assuming the mean delay time of 30 s to penetrate with cutting torch, passive camera. $P_D = 0.15$.

  Total delay time would be 35 s to enter reactor containment with all these tasks, also assuming a $P_D = 0.5$ from drawing attention within the building.

  Therefore, $\beta_D = (0.875)(0.85)(0.5) = 0.372 \rightarrow P_D = 0.628$.

4. Task 4, from the reactor containment into the critical equipment room

   - DOR: 5 -cm wood pedestrian door with balance magnetic switch and electromagnetic lock assuming the mean delay time of 12 s to penetrate door with fire ax, and additional 3 s to run to the target before the 18 s to set the 10 kg explosive.

The value of P_I for this pathway was calculated with these assumptions, P_D, t_D, RFT using EASI model Excel tool shown in Table 16, and the calculated value of P_I value was 0.43.

Table 17. Calculation of Probability of Interruption for Pathway 3 Using EASI Model.

Estimate of Adversary Sequence Interruption		Probability of Interruption:		0.43		
		Probability of Alarm Communication	System Response Time (in seconds)			
			Mean	Standard Deviation		
		0.9	90	27		
Task	Description	P_D	Location	Delay Time (seconds)		Time Left (seconds)
				Mean	Standard Deviation	
1	Penetrates the Fence	0.7625	FEN	12	3.6	198
2	Run to the concrete wall surface at the left side of the building	0.05	VHD	10	3.0	186
3	Penetrate 15 -cm thick concrete wall using TNT shaped charge to enter into the building	0.975	SUR	1	0.3	176
4	Run to the building	0.025	SUR	5	1.5	44
5	Run around hallway, penetrate 0.75 -cm steel door to enter into the reactor containment area	0.647	DOR	35	10.5	39
6	Run to the reactor containment area		DOR	5	1.5	38
7	Penetrate the 5 -cm wooden door to enter into the critical equipment room		DOR	12	3.6	33
8	Enter into the critical equipment room		DOR	3	0.9	21
9	Sabotage the reactor vessel		Target	18	5.4	18

4. SUMMARY AND CONCLUSIONS

4.1 Summary

The objective of this study was to perform the impact investigation on a reinforced concrete model due to Tri-Nitro Toluene (TNT) shaped charge using a numerical simulation software. In addition, a vulnerability analysis of a PPS was performed to provide the most vulnerable pathway for a hypothetical nuclear research reactor facility if an adversary planned to sabotage the nuclear research reactor facility using TNT shaped charge. ANSYS Simulation Software was used for the numerical simulation. Also, the probability of interruption (P_I) was calculated with the Adversary Sequence Diagram (ASD) for the PPS vulnerability analysis.

In this study, two different types of simulation software codes that can be coupled for the advanced analysis were used within ANSYS Simulation Software system. One was ANSYS Explicit Dynamic STR (Structure) software and the other one was ANSYS AUTODYN software. ANSYS Explicit Dynamic STR software provides suitable solutions of nonlinear dynamic events for a short duration, including a drop and impact testing with low velocity or high velocity, deformation by high pressure, explosion, etc. ANSYS AUTODYN software also provides suitable solutions of nonlinear dynamic events similar to ANSYS Explicit Dynamic STR, but this software is focused on complicated nonlinear dynamic events like high explosions and detailed damage responses of materials such as cracks and fragments.

The reinforced concrete wall was modeled using ANSYS Explicit Dynamic code with dimensions of 1850 mm (L) x 1807 mm (H) x 300 mm (W) using 140 MPa concrete material. The concrete wall was reinforced with 14 mm ø steel bars using 4030 steel material. The

reinforced concrete wall target was located at a distance of 50 meters from a TNT shaped charge design.

Using air, TNT, AL 2024-T4, copper, TNT shaped charges were modeled and simulated using ANSYS AUTODYN code. AL 2024-T4 was used to hold TNT as a cylindrical case, and copper was used for the liner material with a conical shape. The amount of TNT of a shaped charge was calculated by geometry of the explosive material which was a cylinder and the geometry of the liner material which was a cone with its density. 7.64 kg TNT shaped charge was used as a beginning model.

The fragment produced due to 7.64 kg TNT shaped charge was modeled with the reinforced concrete wall model in ANSYS Explicit Dynamic STR code, and all data were transferred to ANSYS AUTODYN code in order to perform the simulation of the impact investigation on the reinforce concrete wall model due to TNT shaped charge. 7.64 kg TNT shaped charge took 27.20 ms with the incident velocity of 2039.9 m/s in order to create an impact on the reinforced concrete model. The fragment was able to penetrate fully, and it created a hole on the reinforced concrete model. The size of the hole was 86 mm at the front size and103 mm at the back side.

The resulted hole size was not enough for a person to pass through, therefore parametric studies were performed using 7.64 kg TNT shaped charge by increasing horizontal length or vertical length, and thickness of liners. The parametric study of the horizontal length increase resulted in increasing the length of the fragments and the incident velocity as the horizontal length of TNT shaped charge was increased, however the diameter of the fragments was same. From the parametric study of the vertical length increase, the diameter of the fragments were increased and the length of the fragments was slightly increased, however the incident velocity

considered a constant as the vertical length was increased. The parametric study of increasing

thickness of liners resulted in the largest fragment size, however the incident velocity was

decreased as the thickness of liner was increased.

With these parametric studies, the final design of TNT was modeled and simulated with

increased the horizontal length, the vertical length, and thickness of liners. From the parameter

study of the horizontal length increase, the horizontal length of 400 mm was chosen. Also, the

vertical length of 273 mm was chosen from the parametric study of the vertical length increase.

This was because the resulted hole size in the horizontal length and the vertical length was the

largest hole size. Only the variables for the final design was the thickness of liners which was 9.0

mm, 13.5 mm, 18.5 mm, and 22.0 mm. The calculated amount of TNT was 143.35 kg, and the

thickness of 22.0 mm was chosen for the final design of TNT shaped charge. This model created

a big enough size of hole for a person to pass which was 342 mm at the front side and 364 mm at

the back side.

The vulnerability analysis was performed assuming that the adversary will use TNT

shaped charge in order to sabotage the hypothetical nuclear research reactor facility. There were

three possible pathways to be considered within the hypothetical nuclear reactor facility. The

ASD for each case was created to investigate for minimizing task times and probability of

detection for the adversary, and then the probability of interruption was calculated using EASI

model Excel. The calculated values for each pathway were 0.70, 0.76, and 0.43. From the results,

the most vulnerable pathway to the hypothetical nuclear research reactor would be with the

calculated value of the probability was at 0.43 if an adversary tried to sabotage the nuclear

facility using TNT based shaped charge, which shows a substantial vulnerability of the PPS.

4.2 Conclusions

In conclusion, a hypothetical nuclear research reactor facility was used to perform a vulnerability assessment within this study if an adversary used TNT shaped charge in order to sabotage the nuclear reactor facility. TNT shaped charge could be used to penetrate the reinforced concrete wall for minimizing tasks in order to approach to the desired target within the research reactor building even if the probability of detection would be high. Also, the vulnerability assessment could provide the most vulnerable paths within the research reactor building. These vulnerability assessments of the PPS was made possible through the parametric studies using ANSYS AUTODYN code of impact on the concrete if the adversary used TNT based shaped charge. Therefore, it would be important to strengthen nuclear security and predict the blast load or its impact correctly on the structures that can be used in a nuclear facility. This was because terrorists could weaken a nuclear facility's PPS using direct explosions, other explosive devices, bullets, or linear shaped charges. As a result of these, breaking into the facility could occur and the related harmful effects including the release of high levels of radioactivity. In addition, it could be an avenue for adversaries to steal special nuclear material to make nuclear explosive devices after the adversaries attack or sabotage the nuclear facility.

REFERENCES

1   Fredrik Johnsson-Bengt Vretblad-Åke Sivertun, "Shaped Charge Calculation Models For Explosive Ordnance Disposal Operations." Journal Of Military Studies 2012 Introduction to Shaped Charge

2   William Walters, "Introduction to Shaped Charges." Army Research Laboratory, ARL-SR-150, March 2007

3   Dennis Baum, "Shaped Charge Technology." [https://str.llnl.gov/str/Baum.html]

4   Ahmed M, Qadeer Malik A, "A Review of Works on Shaped Charges." Technology & Applied Science Research 2017 vol: 7 (5) pp: 2098-2103

5   Tamer Abd Elazim Elshenawy, "CRITERIA OF DESIGN IMPROVEMENT OF SHAPED CHARGES USED AS OIL WELL PERFORATORS" (2012).Doctoral Dissertations.

6   Dahana.id, "Explosive Manufacturing of Shaped Charges in Business Line." http://www.dahana.id/business-line/explosive-manufacturing/shaped-charges/

7   Innovative Defense, "Innovative Defense Charge created 2.5" diameter hole." http://innovativedefense.net/investors.php

8   Riedel W. (2009) 10 Years RHT: A Review of Concrete Modelling and Hydrocode Applications. In: Hiermaier S. (eds) Predictive Modeling of Dynamic Processes. Springer, Boston

9   Guendouz K, Sayhi A, Cheng W, "Autodyn-2D Simulation of Shaped Charge Jet Formation and Penetration Mechanism into Multi-Layered Shielded Target." Applied Mechanics and Materials, Trans Tech Publications, Switzerland Vol. 664 (2014) pp 128-137

10   Amir H. Abbassi, "General Birkhoff's Theorem." Department of Physics, School of Sciences, Tarbiat Modarres University

11   Juraj Králik, "Safety Of Nuclear Power Plants Against the Aircraft Attack." Applied Mechanics and Materials 2014

12   Galuta E Regig W, "Numerical Simulations of RC Panels Subjected to High Speed Projectile-Erosion Selection in AUTODYN-3D code." IJISET-International Journal of Innovative Science, Engineering & Technology 2017 vol: 4

13   ANSYS AUTODYN User's Manual Theoretical manual 2005, ANSYS Inc. Southpointe, 2600 ANSYS Drive, Canonsburg, PA, 15317 USA

14   Zatorski Z, "Experimental verification of numerical simulation of projectile impact on ballistic shields." Archive of Mechanical Engineering 2013

15   Saroha D, Kumar D, Singh Y, "Penetration Behaviour Simulation of Shaped Charge Jets in Water Filled Targets."

16   Sheikh Zakir, Li Yulong, Ahmed Sohail, Uzair Dar, Muhammad Rasheed, Atiqa Bibi, "Numerical Study on the Optimum Design Of Explosively Formed Projectile." 2018 15th International Bhurban Conference

17   Brannon R Leelavanichkul S, "Survey of Four Damage Models for Concrete." SANDIA National Laboratories REPORT, 2009

18   S. Austin, A. D. Brown, J. P. Escobedo, H Wang, H. Kleine, P. J. Hazell, "The high-velocity impact of Dyneema® and Spectra® laminates: implementation of a simple thermal softening model." Procedia Engineering 204 (2017) 51–58

19   Xiaohua Zhao, Gaohui Wang, Wenbo Lu, Peng Yan, Ming Chen, Chuangbing Zhou, "Damage Features Of RC Walls Subjected To Air and Underwater Contact Explosions." Ocean Engineering 147 (2018) 531-545

20   Kalia, Hemendra Nath, "Penetration in granite by shaped charge liners of various metals" (1970).Doctoral Dissertations. 2038. http://scholarsmine.mst.edu/doctoral_dissertations/2038HEMENDRA NATH

21   Wu J, Liu J, Du Y, "Experimental and numerical study on the flight and penetration properties of explosively-formed projectile" International Journal of Impact Engineering 2007

22   Sunil Chirayath, "Private communication at Texas A&M University" Director, Center for Nuclear Security Science & Policy Initiatives, Associate Professor, Nuclear Engineering Department, Texas A&M University, College Station, TX 77843-3133, USA

23   GARCIA M. L., "The Design and Evaluation of Physical Protection Systems" Butterworth Heinemann, Boston, Second Edition (2008).

24   Gerald Neville, "Concrete Manual: Based on the 2015 Ibc and Aci 318-14 Concrete Quality and Field Practices" Icc Publications – 2015 https://shop.iccsafe.org/media/wysiwyg/material/9090S15-Sample.pdf